Dispersing billiards with cusps: slow decay of correlations

N. Chernov[*] and R. Markarian[†]

April 3, 2006

Abstract

Dispersing billiards introduced by Sinai are uniformly hyperbolic and have strong statistical properties (exponential decay of correlations and various limit theorems). However, if the billiard table has cusps (corner points with zero interior angles), then its hyperbolicity is nonuniform and statistical properties deteriorate. Until now only heuristic and experiments results existed predicting the decay of correlations as $\mathcal{O}(1/n)$. We present a first rigorous analysis of correlations for dispersing billiards with cusps.

1 Introduction

A billiard is a mechanical system in which a point particle moves in a compact container $\mathcal{D}$ and bounces off its boundary $\partial\mathcal{D}$; in this paper we only consider planar billiards, where $\mathcal{D} \subset \mathbb{R}^2$ or $\mathcal{D} \subset \mathrm{Tor}^2$. The billiard dynamics preserves a uniform measure on its phase space, and the corresponding collision map (generated by the collisions of the particle with $\partial\mathcal{D}$, see below) preserves a natural (and often unique) absolutely continuous measure on its own phase space, see definitions in Section 2. The dynamical properties of a billiard are

[*]Department of Mathematics, University of Alabama at Birmingham, Birmingham, AL 35294, USA; E-mail: chernov@math.uab.edu

[†]Instituto de Matemática y Estadística "Prof. Ing. Rafael Laguardia", Facultad de Ingeniería, Universidad de la República, C.C. 30, Montevideo, Uruguay

determined by the shape of the boundary $\partial\mathcal{D}$, and it may vary greatly from completely regular (integrable) to strongly chaotic.

The first class of chaotic billiards was introduced by Ya. Sinai in 1970 [Si70]; he proved that if the boundary $\partial\mathcal{D}$ of a domain $\mathcal{D} \subset \mathrm{Tor}^2$ is smooth and strictly convex inward (with nowhere vanishing curvature), then the billiard map and flow are hyperbolic (moreover, uniformly hyperbolic), ergodic, mixing and K-mixing. He called such systems *dispersing billiards*, now they are often called *Sinai billiards*. In 1974, Gallavotti and Ornstein [GO74] proved that Sinai's billiards were Bernoulli systems.

Sinai's billiards have strong statistical properties – exponential decay of correlations for the collision map [Y98], central limit theorem and weak invariance principle (for both map and flow, see [BS81, BSC91]), as well as strong invariance principle for the map [C06b].

All these results have been extended to dispersing billiards with piecewise smooth boundary, where corner points exist, provided the interior angles made by the boundary at corner points are all positive [BSC91, C99].

On the contrary, dispersing billiards with corner points with zero internal angles ('cusps') are much harder to investigate; the main reason is a weak (non-uniform) hyperbolicity of the collision map. Indeed, whenever the moving particle gets deep into a cusp, it experiences a large number of rapid collisions that do not contribute much to the expansion or contraction of tangent vectors. Only in 1995, Reháček proved that dispersing billiards with cusps were ergodic [R95], which implied K-mixing by a general argument, see [Si70] and also [CM06, Chapter 6], and Bernoulli property [CH96, OW98].

Statistical properties of dispersing billiards with cusps appear to be similar to those of expanding interval maps with indifferent fixed points (see, for example, [CGS92, CG93, Y99]). Just like a trajectory in an interval may be trapped in a vicinity of an indifferent fixed point, the billiard particle may be trapped in a cusp. Such phenomena result in an intermittent character of the dynamics (switching between regularity and chaos) and they are notoriously hard to analyze.

In 1983, Machta [Mac83] investigated the rate of the decay of correlations for one particular billiard table made by three identical circular arcs tangent to each other at their points of contact (Fig. 1). He argued that correlation function $\mathbf{C}_n(f,g)$, see definitions in the next section, should decay as $\mathcal{O}(1/n)$, which was much slower than the exponential decay then expected (and now established) for dispersing billiards without cusps. Machta's arguments were almost entirely heuristic (he approximated the motion of the billiard particle

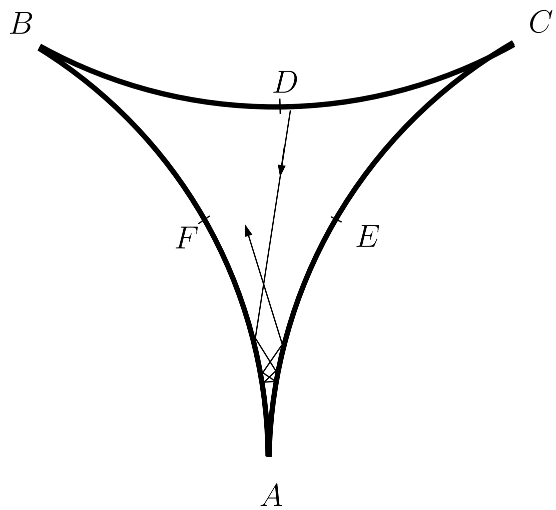

Figure 1: Billiard table with three cusps.

in a cusp by a carefully constructed system of differential equations), but his analysis clearly demonstrated that the dynamics in a cusp were pretty complicated. Machta supported his conjecture by numerical experiments (see also [MR86]).

The (rather unexpected) complexity of the dynamics in a cusp held back the mathematical studies of such billiards for quite a while. Only now we are able to prove Machta's conjecture (in a slightly weaker form):

Theorem 1.1. *For dispersing billiards with cusps, the correlations* $\mathbf{C}_n(f,g)$ *for the collision map and Hölder continuous observables* f,g *are bounded by* $|\mathbf{C}_n(f,g)| \leq C(\ln n)^2/n$*, where* $C > 0$ *is a constant.*

In most of our paper we deal with Machta's three-arc table shown on Fig. 1. This allows us to present the arguments in a fairly tractable and geometrically transparent manner. In Section 6 we describe changes necessary for proving the theorem in the general case.

Remark. Bounds on correlations similar to ours (with a logarithmic factor) have been established for Bunimovich's stadium and other billiard models with polynomial decay of correlations [Mar04, CZ05a]. It is believed that the logarithmic factor is just an artefact of the method used, and a sharp bound on correlations is expected to be C/n. A work is currently underway to improve the argument and eliminate the logarithmic factor.

REMARK. In the studies of hyperbolic maps, if correlations decay as $\mathcal{O}(1/n)$, as in our case, the central limit theorem (CLT) usually fails. However, there are non-classical versions of the CLT that sometimes hold [BG06].

2 Generalities

Here we provide necessary facts from the theory of chaotic billiards. For a more detailed presentation of these and related facts see [BSC90, BSC91, C06a], as well as our recent book [CM06].

A planar billiard is a dynamical system where a point (particle) moves freely at unit speed in a domain $\mathcal{D} \subset \mathbb{R}^2$ and reflects off its boundary $\partial\mathcal{D}$ by the rule "the angle of incidence equals the angle of reflection". It is commonly assumed that $\partial\mathcal{D}$ is a finite union of C^3 curves (arcs). The phase space of this system is a three dimensional manifold $\Omega = \mathcal{D} \times S^1$. The motion of the particle generates a Hamiltonian flow on Ω preserving a Liouville measure, which is a product of uniform measures on $\mathcal{D}$ and S^1.

Let $\mathcal{M} = \partial\mathcal{D} \times [-\pi/2, \pi/2]$ be the standard cross-section of the billiard dynamics, we call $\mathcal{M}$ the *collision space*. Canonical coordinates on $\mathcal{M}$ are r and φ, where r is the arc length parameter on $\partial\mathcal{D}$ and $\varphi \in [-\pi/2, \pi/2]$ is the angle between the postcollisional velocity vector v and the inward normal vector n to $\partial\mathcal{D}$; the orientation of r and φ is shown on Fig. 2.

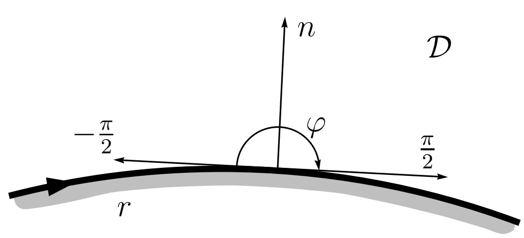

Figure 2: Orientation of r and φ

The first return map $\mathcal{F}\colon \mathcal{M} \to \mathcal{M}$ is called the *collision map* or the *billiard map*, it preserves smooth measure $d\mu = \cos\varphi \, dr \, d\varphi$ on $\mathcal{M}$.

Let $f, g \in L^2_\mu(\mathcal{M})$ be two functions. Correlations are defined by

$$\mathbf{C}_n(f,g) = \int_{\mathcal{M}} (f \circ \mathcal{F}^n)\, g\, d\mu - \int_{\mathcal{M}} f\, d\mu \int_{\mathcal{M}} g\, d\mu. \tag{2.1}$$

It is well known that $\mathcal{F} : \mathcal{M} \to \mathcal{M}$ is *mixing* if and only if

$$\lim_{n\to\infty} \mathbf{C}_n(f,g) = 0 \qquad \forall f, g \in L^2_\mu(\mathcal{M}). \tag{2.2}$$

The rate of mixing of $\mathcal{F}$ is characterized by the speed of convergence in (2.2) for smooth enough functions f and g. We will always assume that f and g are Hölder continuous or piecewise Hölder continuous with singularities that coincide with those of the map $\mathcal{F}^k$ for some k. For example, the free path between successive reflections is one such function.

We say that correlations decay *exponentially* if $|\mathbf{C}_n(f,g)| <$ const $\cdot\, e^{-cn}$ for some $c > 0$ and *polynomially* if $|\mathbf{C}_n(f,g)| <$ const $\cdot\, n^{-a}$ for some $a > 0$. Here the constant factor depends on f and g, but the exponent c (or a) only depends on the map and on the Hölder exponent of the functions f and g. Systems with strong (uniform) hyperbolicity are usually characterized by exponential decay of correlations; systems with weak (nonuniform) hyperbolicity usually have slow (polynomial) mixing rates.

A general strategy for estimating the correlation function $\mathbf{C}_n(f,g)$ for systems with weak hyperbolicity was developed in [CZ05a], it is based on recent Young's results [Y98, Y99] and [Mar04]. That scheme is particularly convenient for billiards.

First, one needs to 'localize' spots in the phase space where expansion (contraction) of tangent vectors slows down. Let $\mathcal{M}_0$ denote the union of all such spots and $\hat{\mathcal{M}} = \mathcal{M} \setminus \mathcal{M}_0$. One needs to verify that the return map $\hat{\mathcal{F}} \colon \hat{\mathcal{M}} \to \hat{\mathcal{M}}$ (that avoids all the 'bad' spots) is strongly (uniformly) hyperbolic. It preserves the measure $\hat{\mu}$ obtained by conditioning μ on $\hat{\mathcal{M}}$. For any $x \in \hat{\mathcal{M}}$ we call

$$R(x) = \min\{n \geq 1 \colon \mathcal{F}^n(x) \in \hat{\mathcal{M}}\}$$

the *return time.*

For dispersing billiards with cusps, hyperbolicity deteriorates only as the moving particle gets deep down a cusp, where it experiences a large number of rapid collisions. We fix $K_0 \gg 1$ and call any sequence of successive collisions of length $> K_0$ in a cusp a *corner series.* We thus define $\mathcal{M}_0$ to be the set of all collision points during those corner series.

Next the strategy developed in [CZ05a] consists of two steps; they are fully described in [CZ05a] (as well as applied to several classes of billiards with slow mixing rates), so we will not bring up unnecessary details here.

At the first step one proves that the return map $\hat{\mathcal{F}}\colon \hat{\mathcal{M}} \to \hat{\mathcal{M}}$ has exponential decay of correlations. At the second step one obtains the following tail bound on the return time function:

$$\hat{\mu}(x \in \hat{\mathcal{M}}\colon R(x) > n) \leq \text{const} \cdot n^{-a} \tag{2.3}$$

for some $a > 1$ and large $n \geq 1$. This usually requires dividing $\hat{\mathcal{M}}$ into the sets $E_n = \{x\colon R(x) = n + 1\}$ and estimating the measure $\hat{\mu}(E_n)$ for large n.

Lastly one uses the following theorem proven in [CZ05a, Section 3]:

Theorem 2.1. *Suppose the map $\hat{\mathcal{F}}\colon \hat{\mathcal{M}} \to \hat{\mathcal{M}}$ has exponential decay of correlations. If the tail bound (2.3) holds for the return time $R(x)$, then correlations are bounded by $|\mathbf{C}_n(f, g)| \leq \text{const}\, (\ln n)^a\, n^{a-1}$.*

3 Corner series

Here we study the geometry of corner series. We examine a billiard trajectory entering a cusp and experiencing a large number of reflections there before getting out. To simplify our analysis we consider here a cusp made by two circular arcs of unit radius with a common tangent line.

Let N be the number of reflections in the corner series and (r_n, φ_n), $1 \leq n \leq N$, denote the all points of reflection in the cusp. We will also work with more convenient coordinates: $\gamma_n = \pi/2 - |\varphi_n|$ and $\alpha_n = |r_n - \bar{r}|$, where $\bar{r}$ stands for the r coordinate of the vertex of the cusp (hence α_n is the length of the arc of $\partial\mathcal{D}$ between the vertex and the nth collision point).

Observe that γ_n are non-negative (in fact $\gamma_n > 0$ for $2 \leq n \leq N - 1$); α_n are all positive; α_n are all small; γ_n are initially small, then slowly grow to about $\pi/2$ (for $n \approx N/2$, as we prove below), and then again decrease and get small for $n \approx N$.

We first show that our trajectory comes closest to the vertex nearly in the middle of the corner series. Let

$$\alpha_{\bar{N}} \colon = \min_n \alpha_n.$$

Lemma 3.1. *We have $|\bar{N} - N/2| \leq 2$.*

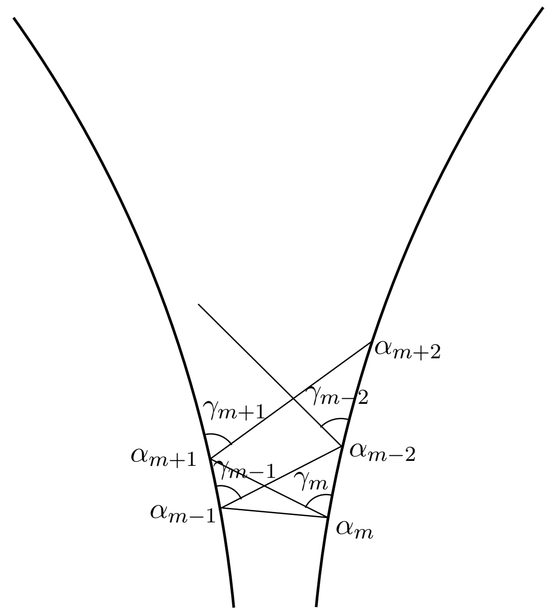

Figure 3: The bottom of a corner series (here $m = \bar{N}$).

Proof. Consider two sequences of points $(\alpha_{\bar{N}+j}, \gamma_{\bar{N}+j})$ and $(\alpha_{\bar{N}-j}, \gamma_{\bar{N}-j})$ for $j = 1, 2, \ldots$. Both sequences are going up, away from the corner, see Fig. 3. Without loss of generality, suppose $\alpha_{\bar{N}+1} \geq \alpha_{\bar{N}-1}$. Then it is clear from Fig. 3 that $\gamma_{\bar{N}+1} \leq \gamma_{\bar{N}-1} \leq \gamma_{\bar{N}}$. It is then an elementary geometric fact that

$$\alpha_{\bar{N}} \leq \alpha_{\bar{N}-1} \leq \alpha_{\bar{N}+1} \leq \alpha_{\bar{N}-2} \leq \alpha_{\bar{N}+2} \leq \cdots$$

and

$$\gamma_{\bar{N}} \geq \gamma_{\bar{N}-1} \geq \gamma_{\bar{N}+1} \geq \gamma_{\bar{N}-2} \geq \gamma_{\bar{N}+2} \geq \cdots \tag{3.1}$$

(note that this is only true if the two circles making the corner are equal).

Therefore, the number of collisions in the corner series occurring before $\bar{N}$ and after $\bar{N}$ differ by no more than one, i.e. $|\bar{N} - N/2| \leq 2$. □

The two halves of the corner series, one before $\bar{N}$ and the other after $\bar{N}$ have very similar structure and properties. It will be enough to study in detail the first half of the series, $0 \leq n \leq \bar{N}$.

We further subdivide the corner series into three segments. We fix a small $\bar{\gamma} \in (0, \pi/2)$ whose exact value is not important, say $\bar{\gamma} = 10^{-10}$. Now let

$$N_1 = \max\{n < \bar{N} \colon \gamma_n \leq \bar{\gamma}\},$$

denote $N_2 = \bar{N}$ and put

$$N_3 = \min\{n > \bar{N} \colon \gamma_n \leq \bar{\gamma}\}.$$

Note that $0 < N_1 < N_2 < N_3 < N$. In what follows we use N_2 instead of $\bar{N}$. We call the segment $[1, N_1]$ the *entering period* in the corner series, the segment $[N_1 + 1, N_3 - 1]$ the *turning period* in it, and the segment $[N_3, N]$ its *exiting period*. It follows from (3.1) that $|N_1 - N_3| \leq 2$.

CONVENTION. We use the following notation: $A \asymp B$ means that $C^{-1} < A/B < C$ for some constant $C = C(\mathcal{D}) > 0$. Also, $A = \mathcal{O}(B)$ means that $|A|/B < C$ for some constant $C = C(\mathcal{D}) > 0$.

Proposition 3.2. *We have*

$$N_1 \asymp N_2 - N_1 \asymp N_3 - N_2 \asymp N - N_3 \asymp N,$$

hence all the three segments in the corner series have length of order N. Also,

$$\alpha_1 \asymp N^{-2/3} \qquad \text{and} \qquad \alpha_{N_2} \asymp N^{-1}, \tag{3.2}$$

and

$$\alpha_n \asymp n^{-1/3} N^{-2/3} \qquad \forall n = 2, \ldots, N_1 \tag{3.3}$$

Also,

$$\gamma_1 = \mathcal{O}(N^{-2/3}) \qquad \text{and} \qquad \gamma_2 \asymp N^{-2/3} \tag{3.4}$$

and

$$\gamma_n \asymp n\alpha_n \asymp n^{2/3} N^{-2/3} \qquad \forall n = 2, \ldots, N_1. \tag{3.5}$$

Proof. We consider the first half of the series, $1 \leq n \leq N_2$. The following equations are simple geometric facts:

$$\gamma_{n+1} = \gamma_n + (\alpha_n + \alpha_{n+1}) \tag{3.6}$$

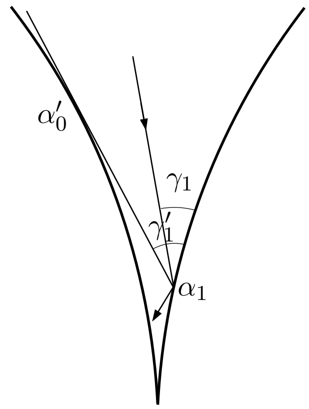

Figure 4: The first collision in a corner series.

and

$$\sin\alpha_{n+1} = \sin\alpha_n - \frac{2 - \cos\alpha_n - \cos\alpha_{n+1}}{\tan(\gamma_n + \alpha_n)}. \tag{3.7}$$

Due to (3.6) we have

$$\gamma_2 = \gamma_1 + \alpha_1 + \alpha_2 \geq 2\alpha_2 \tag{3.8}$$

and

$$\gamma_1 + \alpha_1 + 2\alpha_2 + \cdots + 2\alpha_{n-2} + \alpha_{n-1} = \gamma_n \leq \pi/2$$

hence

$$\alpha_1 + \cdots + \alpha_n \leq \pi/2 \tag{3.9}$$

for all $n \leq N_2$.

At the very first collision, we have $\gamma_1 < \gamma_1'$, where γ_1' denotes the angle made by the line passing through the first collision point and tangent to the other arc (Fig. 4). If we denote by α_0' the coordinate of the point of tangency, then equations (3.6)–(3.7) take form

$$\gamma_1' = \alpha_0' + \alpha_1, \qquad \sin\alpha_1 = \sin\alpha_0' - \frac{2 - \cos\alpha_0' - \cos\alpha_1}{\tan\alpha_0'}.$$

This easily gives $\alpha_1/\alpha_0' \to 1 + \sqrt{2}$, as $N \to \infty$, hence

$$\gamma_1 < \gamma_1' = (2 + \sqrt{2} + o(1))\,\alpha_1 \leq 4\alpha_1. \tag{3.10}$$

We introduce new variables:

$$u_n = \frac{\alpha_{n+1}}{\alpha_n} \quad \text{and} \quad w_n = \frac{\gamma_n}{\alpha_n},$$

hence

$$\alpha_n = \alpha_1 u_1 u_2 \cdots u_{n-1}. \tag{3.11}$$

It is important to find the asymptotics for w_n. Equation (3.6) yields

$$w_{n+1} = 1 + \frac{w_n + 1}{u_n} \tag{3.12}$$

Since $u_n \leq 1$, we have $w_{n+1} \geq w_n + 2$. Since $w_2 \geq 2$ by (3.8), we obtain a lower bound for w_n:

$$w_n \geq 2n - 2. \tag{3.13}$$

To get an upper bound for w_n, we first use (3.7) and obtain

$$\begin{aligned} \alpha_{n+1} &> \alpha_n - \frac{\alpha_n^3}{6} - \frac{2 - (1 - \alpha_n^2/2) - (1 - \alpha_{n+1}^2/2)}{\gamma_n + \alpha_n} \\ &= \alpha_n - \frac{\alpha_n^3}{6} - \frac{\alpha_n^2 + \alpha_{n+1}^2}{2(\gamma_n + \alpha_n)} \end{aligned}$$

This is equivalent to

$$u_n > 1 - \frac{\alpha_n^2}{6} - \frac{1 + u_n^2}{2(1 + w_n)} > 1 - \frac{\alpha_n^2}{6} - \frac{1}{1 + w_n} \tag{3.14}$$

Combining this with (3.12) gives

$$w_{n+1} < 1 + \frac{w_n + 1}{1 - \frac{\alpha_n^2}{6} - \frac{1}{w_n + 1}}$$

Note that $1/(1-x) < 1 + x + 2x^2$ for small positive x (in fact, for all $0 < x < 1/2$; and we indeed have $\alpha_n^2/6 + 1/(w_n + 1) < 1/2$ since α_n are all small and $w_n \geq 2$). Using this fact and making simple calculation yields

$$w_{n+1} < w_n + 3 + \alpha_n^2 w_n + \frac{4}{w_n + 1} + \alpha_n^4 (w_n + 1) \tag{3.15}$$

The lower bound (3.13) now implies

$$w_n < 3n + 2\ln n + 2\sum_{i=0}^{n-1} \alpha_i^2 w_i + C$$

for some absolute constant C (we note that $w_1 \le 4$ due to (3.10)). The bound (3.9) implies

$$\sum_{i=1}^{n} \alpha_i^2 w_i = \sum_{i=1}^{n} \alpha_i \gamma_i \le \frac{\pi}{2}\sum_{i=1}^{n} \alpha_i \le \frac{\pi^2}{4} \tag{3.16}$$

hence

$$w_n < 3n + 2\ln n + C \tag{3.17}$$

We will denote by C absolute constants (possibly different in different equations) whose exact values are not important. Now we have an upper bound for w_n, and the overall asymptotic is $w_n \asymp n$. In particular, as a result of (3.13) and (3.17) and the obvious $\gamma_{N_2} \approx \pi/2$ we have

$$\frac{\pi}{6N_2 + 4\ln N_2 + 2C} < \alpha_{\min} < \frac{\pi}{4N_2} \tag{3.18}$$

Next we focus on the entering period, i.e. on $1 \le n \le N_1$. As long as $\gamma_n \le \bar{\gamma}$ we have

$$\tan(\gamma_n + \alpha_n) < \gamma_n + \alpha_n + \bar{c}(\gamma_n + \alpha_n)^3$$

where $\bar{c} > 0$ is a constant determined by $\bar{\gamma}$. Now the equation (3.7) yields

$$\alpha_{n+1} - \frac{\alpha_{n+1}^3}{6} < \alpha_n - \frac{\alpha_n^2/2 - \alpha_n^4/24 + \alpha_{n+1}^2/2 - \alpha_{n+1}^4/24}{\gamma_n + \alpha_n + \bar{c}(\gamma_n + \alpha_n)^3}$$

Note that $\alpha_{n+1} - \alpha_{n+1}^3/6 > \alpha_{n+1}(1 - \alpha_n^2/6)$, hence

$$\alpha_{n+1} < \left[\alpha_n - \frac{\alpha_n^2 + \alpha_{n+1}^2 - \alpha_n^4/6}{2(\gamma_n + \alpha_n) + 2\bar{c}(\gamma_n + \alpha_n)^3}\right] \Big/ \left[1 - \frac{\alpha_n^2}{6}\right]$$

or, equivalently,

$$u_n < \left[1 - \frac{1 + u_n^2 - \alpha_n^2/6}{2(w_n + 1) + 8\bar{c}(w_n + 1)\gamma_n^2}\right] \Big/ \left[1 - \frac{\alpha_n^2}{6}\right]. \tag{3.19}$$

We now substitute (3.19) into (3.12) and after simple calculation arrive at

$$w_{n+1} > 2 + w_n + (1+u_n^2)/2 - 8\bar{c}\gamma_n^2 - w_n\alpha_n^2.$$

Then we use the estimate (3.14) of u_n and, with some more simple calculation, obtain

$$\begin{aligned} w_{n+1} &> 3 + w_n - (w_n+1)^{-1} - (w_n+1)^{-2} - 8\bar{c}\gamma_n^2 - 2w_n\alpha_n^2 \\ &> 3 + w_n - (2n)^{-1} - (2n)^{-2} - 8\bar{c}\gamma_n^2 - 2w_n\alpha_n^2, \end{aligned} \tag{3.20}$$

where we also used (3.13).

We now combine (3.12), (3.20) and (3.17):

$$\begin{aligned} u_n^{-1} &= \frac{w_{n+1}-1}{w_n+1} \\ &> 1 + \frac{1-(2n)^{-1}-(2n)^{-2}-8\bar{c}\gamma_n^2-2w_n\alpha_n^2}{w_n+1} \\ &> 1 + \frac{1-(2n)^{-1}-(2n)^{-2}-8\bar{c}\gamma_n^2-2w_n\alpha_n^2}{3n+2\ln n+C} - 2\alpha_n^2 \\ &> 1 + \frac{1}{3n+2\ln n+C} - \frac{1}{n^2} - \frac{8\bar{c}\gamma_n^2}{n} - 2\alpha_n^2. \end{aligned}$$

Observe that $1+x > e^{x-x^2}$ for small x, hence, with some simple calculation, we obtain

$$u_n^{-1} > \exp\left(\frac{1}{3n+2\ln n+C} - \frac{2}{n^2} - \frac{8\bar{c}\gamma_n^2}{n} - 2\alpha_n^2 - \frac{4\bar{c}^2\gamma_n^2}{n^2} - \frac{64\bar{c}^2\gamma_n^4}{n^2}\right) \tag{3.21}$$

or, lastly,

$$\prod_{i=1}^n u_i^{-1} > \exp\left(\sum_{i=1}^n \frac{1}{3i+2\ln i+C} - \sum_{i=1}^n \frac{2}{i^2} - \sum_{i=1}^n \frac{8\bar{c}\gamma_i^2}{i} - 2\sum_{i=1}^n \alpha_i^2 - \sum_{i=1}^n \frac{100\bar{c}^2\gamma_i^4}{i^2}\right) \tag{3.22}$$

Note that by (3.17) and (3.16)

$$\sum_{i=1}^n \frac{\gamma_i^2}{i} < 8\sum_{i=1}^n \frac{\gamma_i^2}{w_i} < 8\sum_{i=1}^n \alpha_i\gamma_i < 2\pi^2$$

and similarly

$$\sum_{i=1}^n \frac{\gamma_i^4}{i^2} < 64\sum_{i=1}^n \frac{\gamma_i^4}{w_i^2} < 64\sum_{i=1}^n \alpha_i^2\gamma_i^2 < 16\pi^2\sum_{i=1}^n \alpha_i^2 < 8\pi^3.$$

By a simple calculation

$$\sum_{i=1}^{n} \frac{1}{3i + 2\ln i + C} = \frac{1}{3}\ln n + \Delta_n$$

where $|\Delta_n| <$const is bounded. Therefore, (3.22) has a shorter form:

$$\prod_{i=1}^{n} u_i^{-1} > \exp\left(\frac{1}{3}\ln n - C\right) \tag{3.23}$$

where $C > 0$ is a constant. Combining this with (3.11) gives

$$\alpha_n < Cn^{-1/3}\alpha_1 \tag{3.24}$$

for all $1 \le n \le N_1$.

We now estimate α_n from below in a similar way. By (3.20)

$$w_n > 3n - \ln n - 2\bar{c}\sum_{i=1}^{n} \gamma_i^2 - C$$

for some constant $C > 0$, where (3.16) was used. For brevity, denote

$$\Gamma_n = \sum_{i=1}^{n} \gamma_i^2.$$

We now use (3.14) and the obvious fact $(1-x)^{-1} < 1 + 2x$ for small positive x and arrive at

$$u_n > 1 - \frac{1}{3n} - \frac{\alpha_n^2}{6} - \frac{2\ln n}{9n^2} - \frac{2C}{9n^2} - \frac{4\bar{c}\Gamma_n}{9n^2}. \tag{3.25}$$

Using another obvious fact, $1 - x > e^{-x-x^2}$ (for small x), we obtain

$$u_1 \cdots u_n > \exp\biggl(-\frac{1}{3}\ln n - C - \sum_{i=1}^{n} \frac{4\bar{c}\Gamma_i}{9i^2}\biggr). \tag{3.26}$$

We now show that $\sum_{i=1}^{n} \Gamma_i/i^2$ is bounded. Indeed,

$$\sum_{i=1}^{n} \frac{\Gamma_i}{i^2} = \sum_{i=1}^{n}\sum_{j=1}^{i} \frac{\gamma_j^2}{i^2} = \sum_{j=1}^{n}\sum_{i=j}^{n} \frac{\gamma_j^2}{i^2} < 2\sum_{j=1}^{n} \frac{\gamma_j^2}{j}$$

Since $\gamma_j = w_j\alpha_j$, using (3.17) gives

$$\sum_{i=1}^{n} \frac{\Gamma_i}{i^2} < C \sum_{j=1}^{n} \gamma_j\alpha_j$$

for some constant $C > 0$. The last expression is bounded by (3.9).

Now combining (3.11) with (3.26) gives $\alpha_n > Cn^{-1/3}\alpha_1$ for all $1 \le n \le N_1$, with some $C > 0$. Along with (3.24) this gives $\alpha_n \asymp n^{-1/3}\alpha_1$ for all $n \le N_1$. Since $\gamma_{N_1} \approx \bar{\gamma} =$const, the bounds (3.13) and (3.17) give $N_1 \asymp \alpha_1^{-3/2}$.

We now consider the turning period, where $N_1 \le n \le N_2$, then the angle γ_n grows from $\bar{\gamma}$ to about $\pi/2$. First, note that

$$\alpha_n = \gamma_n/w_n > \bar{\gamma}/(3n + \ln n + C).$$

By (3.6) we have

$$\sum_{n=N_1}^{N_2} (\gamma_n - \gamma_{n-1}) \ge \sum_{n=N_1}^{N_2} \frac{C'}{3n + \ln n + C} \ge C'' \ln \frac{N_2}{N_1}$$

for some constants $C', C'' > 0$. Therefore, $N_1 < N_2 < CN_1$ for some $C > 0$. We then obtain $\alpha_1^{-3/2} \asymp N_2 \asymp N$, and for $\alpha_{N_2} = \min_n \alpha_n$ we have $\alpha_{N_2} \asymp N_2^{-1/3}\alpha_1 \asymp N^{-1/3}\alpha_1$. The proposition is proved. $\square$

For our future use we record some estimates obtained in the proof for the entering period of the corner series, i.e. for $1 \le n \le N_1$. Due to (3.15) and (3.20) we have

$$w_{n+1} - w_n = 3 + \mathcal{O}(n^{-1} + \gamma_n^2) \tag{3.27}$$

(we note that $w_n\alpha_n^2 \asymp n^{1/3}N^{-4/3} = \mathcal{O}(n^{-1})$, so that the term $w_n\alpha_n^2$ is absorbed by others). Observe that $n^{-1} \ll \gamma_n^2$ for small n but $n^{-1} \gg \gamma_n^2$ for $n \approx N_1$, so we have to keep both parts of the $\mathcal{O}(\cdot)$ term in (3.27).

Equation (3.27) immediately implies

$$w_n = 3n + \mathcal{O}(\ln n + \Gamma_n). \tag{3.28}$$

This estimate combined with (3.21) and (3.25) gives

$$u_n = 1 - \frac{1}{3n} + \mathcal{O}\Big(\frac{\ln n}{n^2}\Big) + \mathcal{O}\Big(\frac{\gamma_n^2}{n}\Big) + \mathcal{O}\Big(\frac{\Gamma_n}{n^2}\Big). \tag{3.29}$$

Next, the following sums were proven to be uniformly bounded (by constants independent of $n < N_1$ and N):

$$\sum_{i=1}^{n} \frac{\gamma_i^2}{i} = \mathcal{O}(1) \quad \text{and} \quad \sum_{i=1}^{n} \frac{\Gamma_i}{i^2} = \mathcal{O}(1). \tag{3.30}$$

We will also need asymptotic formulas for the intercollision times during a corner series. Denote by t_n the time of the nth collision, $1 \le n \le N$, and by $\tau_n = t_{n+1} - t_n$ the time between successive collisions. It is a simple geometric fact that

$$\tau_n = \frac{2 - \cos\alpha_n - \cos\alpha_{n+1}}{\sin(\gamma_n + \alpha_n)} \tag{3.31}$$

for all $1 \le n < N_2$ (when the trajectory is going down the corner). Expanding into Taylor series and using (3.3) and (3.28)–(3.29) gives

$$\begin{aligned}
\tau_n &= \frac{\alpha_n}{2w_n}\,\frac{1 + u_n^2 + \mathcal{O}(\gamma_n^2)}{1 + w_n^{-1} + \mathcal{O}(\alpha_n^2 w_n^2)} \\
&= \frac{\alpha_n}{w_n}\,\frac{2 + \mathcal{O}(1/n) + \mathcal{O}(\alpha_n^2)}{2 + \mathcal{O}(1/n) + \mathcal{O}(\gamma_n^2)} \\
&= \alpha_n w_n^{-1}\big(1 + \mathcal{O}(1/n) + \mathcal{O}(\gamma_n^2)\big) \\
&\asymp n^{-4/3} N^{-2/3}.
\end{aligned} \tag{3.32}$$

This gives us another important relation

$$\begin{aligned}
\frac{\tau_n}{\sin\gamma_n} &= \frac{\alpha_n w_n^{-1}\big(1 + \mathcal{O}(1/n) + \mathcal{O}(n^2\alpha_n^2)\big)}{\alpha_n w_n\big(1 + \mathcal{O}(\gamma_n^2)\big)} \\
&= \frac{1}{w_n^2}\left(1 + \mathcal{O}(1/n) + \mathcal{O}(\gamma_n^2)\right) \\
&= \frac{1}{9n^2} + \mathcal{O}\Big(\frac{\ln n}{n^3} + \frac{\gamma_n^2}{n^2} + \frac{\Gamma_n}{n^3}\Big)
\end{aligned} \tag{3.33}$$

We need to estimate the ratio of neighboring τ_n's by using (3.31):

$$\frac{\tau_{n+1}}{\tau_n} = \frac{2 - \cos\alpha_{n+1} - \cos\alpha_{n+2}}{2 - \cos\alpha_n - \cos\alpha_{n+1}} \times \frac{\sin(\gamma_n + \alpha_n)}{\sin(\gamma_{n+1} + \alpha_{n+1})} =: F_n' \times F_n''.$$

The first fraction behaves as

$$\begin{aligned} F'_n &= \frac{\alpha_{n+1}^2(1+u_{n+1}^2)+\mathcal{O}(\alpha_{n+1}^4)}{\alpha_n^2(1+u_n^2)+\mathcal{O}(\alpha_n^4)} \\ &= \frac{u_n^2(1+u_{n+1}^2)+\mathcal{O}(\alpha_{n+1}^2)}{1+u_n^2+\mathcal{O}(\alpha_n^2)} \\ &= 1-\frac{2}{3n}+\mathcal{O}\Big(\frac{\ln n}{n^2}+\frac{\gamma_n^2}{n}+\frac{\Gamma_n}{n^2}+\alpha_n^2\Big), \end{aligned}$$

where we used (3.29) three times. Note that $\mathcal{O}(\alpha_n^2)=\mathcal{O}(\gamma_n^2/n^2)$, hence the last term is actually absorbed by the others. Next

$$\begin{aligned} F''_n &= 1-\frac{\sin(\gamma_{n+1}+\alpha_{n+1})-\sin(\gamma_n+\alpha_n)}{\sin(\gamma_{n+1}+\alpha_{n+1})} \\ &= 1-\frac{[\alpha_n u_n(w_{n+1}+1)-\alpha_n(w_n+1)]\cos\theta}{\alpha_n u_n(w_{n+1}+1)+\mathcal{O}(\gamma_n^3)}, \end{aligned}$$

where $\theta\in(\gamma_n+\alpha_n,\gamma_{n+1}+\alpha_{n+1})$ by the mean value theorem, hence

$$F''_n = 1-\frac{u_n(w_{n+1}+1)-(w_n+1)}{u_n(w_{n+1}+1)}\big(1+\mathcal{O}(\gamma_n^2)\big).$$

According to (3.27), (3.28) and (3.29) the numerator behaves as

$$\begin{aligned} u_n(w_{n+1}+1)-(w_n+1) &= (u_n-1)w_n+4u_n-1+\mathcal{O}(n^{-1}+\gamma_n^2) \\ &= 2+\mathcal{O}\Big(\frac{\ln n}{n}+\gamma_n^2+\frac{\Gamma_n}{n}\Big), \end{aligned}$$

hence

$$F''_n = 1-\frac{2}{3n}+\mathcal{O}\Big(\frac{\ln n}{n^2}+\frac{\gamma_n^2}{n}+\frac{\Gamma_n}{n^2}\Big).$$

Again, $\mathcal{O}(n\alpha_n^2)=\mathcal{O}(\gamma_n^2/n)$, hence the last term is actually absorbed by the others. Combining our estimates for F'_n and F''_n gives

$$\frac{\tau_{n+1}}{\tau_n} = 1-\frac{4}{3n}+\mathcal{O}\Big(\frac{\ln n}{n^2}+\frac{\gamma_n^2}{n}+\frac{\Gamma_n}{n^2}\Big) \tag{3.34}$$

for all $n=1,\dots,N_1$.

During the turning period, where $N_1\le n\le N_3$, we have $\alpha_n\asymp 1/N$ by (3.2) and (3.3). Since $\gamma_n\ge\bar\gamma>0$, we easily obtain $\tau_n\asymp\alpha_n^2\asymp N^{-2}$. Thus the time spent by the trajectory during each period in the corner series has the same order of magnitude:

$$\sum_{n=1}^{N_1-1} \tau_n \asymp 1/N \qquad \text{and} \qquad \sum_{n=N_1}^{N_3} \tau_n \asymp 1/N.$$

Remark 3.3. *Due to the time reversibility of billiard dynamics, all the asymptotic formulas obtained for the entering period remain valid for the exiting period. In particular,*

$$\alpha_N \asymp N^{-2/3} \qquad \textit{and} \qquad \gamma_N = \mathcal{O}(N^{-2/3}). \tag{3.35}$$

During the exiting period we will also use the 'countdown' index $m = N + 1 - n$, so that $m = 1, \dots, N - N_3$; then in all our asymptotic formulas we can simply replace n by m. For example,

$$\alpha_m \asymp m^{-1/3} N^{-2/3} \qquad \textit{and} \qquad \gamma_m \asymp m\alpha_m \asymp m^{2/3} N^{-2/3} \tag{3.36}$$

for all $m = 2, \dots, N - N_3$, etc.

4 Expansion of unstable curves

In this section we estimate the rate of expansion of unstable vectors during corner series. First we recall general facts about unstable tangent vectors in dispersing billiards [BSC90, BSC91, C06a, CM06].

Let $x = (r, \varphi) \in \mathcal{M}$. A tangent vector $dx = (dr, d\varphi) \in \mathcal{T}_x\mathcal{M}$ can be represented by an infinitesimal curve $\gamma = \gamma(s) \subset \mathcal{M}$, where $s \in (-\varepsilon, \varepsilon)$ is a parameter, such that $\gamma(0) = x$ and $\frac{d}{ds}\gamma(0) = dx$.

The trajectories of the points $y \in \gamma$, after leaving $\mathcal{M}$, make a one-parameter family (a bundle) of directed lines in $\partial\mathcal{D}$. The curvature of the orthogonal cross-section of that bundle at x plays an important role; we denote it by $\mathcal{B}^+ = \mathcal{B}^+(x)$. Similarly, the past trajectories of the points $y \in \gamma$ (*before* arriving at $\mathcal{M}$) make a bundle of directed lines in $\partial\mathcal{D}$ whose curvature right before the collision with $\partial\mathcal{D}$ at x is denoted by $\mathcal{B}^-$. We have

$$\mathcal{B}^+ = \mathcal{B}^- + \frac{2\mathcal{K}}{\cos\varphi}, \tag{4.1}$$

where $\mathcal{K} = \mathcal{K}(r)$ denotes the curvature of the boundary $\partial\mathcal{D}$ at the point r. For dispersing billiards $\mathcal{K}$ is positive and bounded away from zero and infinity. The tangent vector dx is said to be unstable if $\mathcal{B}^- > 0$ (hence $\mathcal{B}^+ > 0$ as well). The slope of the vector dx is

$$d\varphi/dr = \mathcal{B}^- \cos\varphi + \mathcal{K} = \mathcal{B}^+ \cos\varphi - \mathcal{K},$$

thus $d\varphi/dr > 0$ for unstable vectors. At the next collision point $x_1 = \mathcal{F}(x) \in \mathcal{M}$, the image vector $dx_1 = D_x\mathcal{F}(dx)$ is characterized by the (precollisional) curvature $\mathcal{B}_1^-$ satisfying

$$\mathcal{B}_1^- = \cfrac{1}{\tau + \cfrac{1}{\mathcal{B}^+}} = \frac{\mathcal{B}^+}{1 + \tau\mathcal{B}^+}, \tag{4.2}$$

where τ is the time between collisions at the points x and $\mathcal{F}(x)$ (it is also the distance between the corresponding collision points, because the moving particle travels at unit speed). Note that $\mathcal{B}^+ > 0$ implies $\mathcal{B}_1^- > 0$, thus the image of an unstable vector will always be an unstable vector.

We measure tangent vectors $dx \in \mathcal{T}_x\mathcal{M}$ in the Euclidean norm

$$\|dx\| = \left[(dr)^2 + (d\varphi)^2\right]^{1/2}$$

For unstable vectors, it is more convenient to use the p-norm defined by

$$\|dx\|_p = \cos\varphi \, dr.$$

The p-norm corresponds to the size of the orthogonal cross-section of the associated bundle of trajectories (it is the same before and after collision). In the p-norm, the expansion of unstable tangent vectors is given by

$$\frac{\|D_x\mathcal{F}(dx)\|_p}{\|dx\|_p} = 1 + \tau\mathcal{B}^+, \tag{4.3}$$

Note that this ratio is > 1, i.e. unstable vectors expand monotonically in the p-norm (this is not necessarily true in the Euclidean norm, see [CM06, Chapter 4]).

We return to our corner series. Again, for simplicity we analyze the three-arc billiard table shown on Fig. 1 and we assume that the arcs have unit radius. Let $x = (r, \varphi) \in \hat{\mathcal{M}}$ be a point whose trajectory $\{\mathcal{F}^i(x)\}_{i=1}^N$ is going down a cusp (say, A) and comes back after N reflections. In that case

$\hat{\mathcal{F}}(x) = \mathcal{F}^{N+1}(x)$, i.e. the return function takes value $R(x) = N+1$. We denote by

$$E_N = \{x \in \hat{\mathcal{M}} \colon R(x) = N+1\}$$

the set of points whose trajectories go down a cusp for a corner series of exactly N collisions. We denote by $x_n = (r_n, \varphi_n) = \mathcal{F}^n(x)$ the images of the point x during the corner series, $1 \le n \le N$, which corresponds to our notation in the previous section.

Obviously, x has to start near the point D (opposite to the cusp A, see Fig. 1) and $\hat{\mathcal{F}}(x) = \mathcal{F}^{N+1}(x)$ has to land back near D again. At the point $x = (r, \varphi)$, we have $\varphi \approx 0$ and $0 < c < \mathcal{B}^- < C$ for some constants $c, C > 0$. Thus $\cos\varphi \asymp 1$ and $0 < d\varphi/dr \asymp 1$, hence the Euclidean norm and the p-norm are uniformly equivalent on unstable vectors at our points $x \in E_N$ and $\hat{\mathcal{F}}(x)$, i.e. right before and right after long corner series.

Given an unstable vector $dx \in \mathcal{T}_x\mathcal{M}$, we denote by $dx_n = (dr_n, d\varphi_n) = D_x\mathcal{F}^n(dx)$ its images. We are interested in the total expansion factor of dx

$$\frac{\|D_x\hat{\mathcal{F}}(dx)\|}{\|dx\|} = \frac{\|D_x\mathcal{F}^{N+1}(dx)\|}{\|dx\|}$$

during the corner series.

Proposition 4.1. *For every $x \in E_N$ the total expansion factor for unstable vectors in the course of the corner series of N collisions has lower bound*

$$\frac{\|D_x\mathcal{F}^{N+1}(dx)\|}{\|dx\|} \ge CN^{5/3}, \tag{4.4}$$

where $C > 0$ is a constant. Its precise asymptotic is

$$\frac{\|D_x\mathcal{F}^{N+1}(dx)\|}{\|dx\|} \asymp N^{5/3}\left(1 + \frac{N^{-2/3}}{\cos\varphi_1}\right)\left(1 + \frac{N^{-2/3}}{\cos\varphi_N}\right) \tag{4.5}$$

Proof. Since the Euclidean norm and the p-norm are uniformly equivalent at the points $x \in E_N$ and $\mathcal{F}^{N+1}(x)$, we can safely replace $\|\cdot\|$ with $\|\cdot\|_p$; then we can use the formula (4.3) at every collision.

Let t_n denote the time of collision at x_n and $\tau_n = t_{n+1} - t_n$ the intercollision time (note that τ_n is the distance between the points of the nth and $(n+1)$st collisions, as the speed of the moving particle equals one). Then the expansion factor for the vector dx under $D_x\mathcal{F}^n$ is

$$\frac{\|D_x\mathcal{F}^n(dx)\|_p}{\|dx\|_p} = \prod_{i=0}^{n-1}(1 + \tau_i\mathcal{B}_i^+) \tag{4.6}$$

where for $\mathcal{B}_n^+$ we have a recursive formula, due to (4.1)–(4.2):

$$\mathcal{B}_{n+1}^+ = \frac{2}{\sin\gamma_{n+1}} + \frac{\mathcal{B}_n^+}{1+\tau_n\mathcal{B}_n^+} \tag{4.7}$$

(remember that $\mathcal{K}=1$ and $\gamma_n = \pi/2 - |\varphi_n|$, so $\cos\varphi_n = \sin\gamma_n$).

Before we proceed, let us make an important remark. Recall that (3.4) and (3.35) only guarantee that $\gamma_1 = \mathcal{O}(N^{-2/3})$ and $\gamma_N = \mathcal{O}(N^{-2/3})$; in fact both γ_1 and γ_N may be arbitrarily close to zero. Thus the expansion of unstable vectors at the very first and the very last collision of the corner series may be arbitrarily strong. On the other hand, (4.7) shows that $\mathcal{B}_{n+1}$ is a monotonically increasing function of both $\mathcal{B}_n^+$ and $1/\sin\gamma_{n+1}$. Thus if we increase γ_1 and γ_N, the total expansion factor $\|D_x\mathcal{F}^{N+1}(dx)\|/\|dx\|$ will only decrease. So we can assume that

$$\gamma_1 \asymp N^{-2/3} \qquad \text{and} \qquad \gamma_N \asymp N^{-2/3} \tag{4.8}$$

and obtain an (asymptotical) lower bound on the total expansion factor. We will actually assume (4.8) and prove that

$$\frac{\|D_x\mathcal{F}^{N+1}(dx)\|_p}{\|dx\|_p} \asymp N^{5/3}. \tag{4.9}$$

This will give us, in particular, (4.4) for all $x \in E_N$.

For $n=0$ we have $\mathcal{B}_0^+ \asymp 1$ and $\tau_0 \asymp 1$, hence $1+\tau_0\mathcal{B}_0^+ \asymp 1$, so the term $i=0$ in (4.6) does not affect the asymptotics. For $n \geq 1$, we put $\lambda_n = \tau_n\mathcal{B}_n^+$, then (4.6) takes form

$$\frac{\|D_x\mathcal{F}^{n}(dx)\|_p}{\|dx\|_p} = \prod_{i=0}^{n-1}(1+\lambda_i) \tag{4.10}$$

and (4.7) takes form

$$\lambda_{n+1} = \frac{2\tau_{n+1}}{\sin\gamma_{n+1}} + \frac{\tau_{n+1}}{\tau_n}\,\frac{\lambda_n}{1+\lambda_n}. \tag{4.11}$$

Lemma 4.2. *For all $x \in E_N$ satisfying (4.8) we have*

$\lambda_n \asymp 1/n$	for	$1 \leq n \leq N_1$	(entering period)
$\lambda_n \asymp 1/n \asymp 1/N$	for	$N_1 \leq n \leq N_3$	(turning period)
$\lambda_n \asymp 1/(N-n)$	for	$N_3 \leq n < N$	(exiting period)

Proof. During the entering period, we have

$$\lambda_{n+1} > \frac{a}{n^2} + \left(1 - \frac{b}{n}\right) \frac{\lambda_n}{1+\lambda_n}$$

for some $a, b > 0$ due to (3.33) and (3.34). Assuming that $\lambda_n > c/n$ we get

$$\begin{aligned} \lambda_{n+1} &> \frac{a}{n^2} + \left(1 - \frac{b}{n}\right) \frac{c/n}{1+c/n} \\ &= \frac{c + (a - bc + ac/n)/n}{n+c}. \end{aligned}$$

If $c > 0$ is small enough, the expression in parentheses is positive and we obtain $\lambda_{n+1} > c/(n+c) > c/(n+1)$, thus completing the induction. Similarly,

$$\lambda_{n+1} < \frac{A}{n^2} + \left(1 - \frac{B}{n}\right) \frac{\lambda_n}{1+\lambda_n}$$

for some $A, B > 0$ due to (3.33) and (3.34). Assuming that $\lambda_n < C/n$ we get

$$\begin{aligned} \lambda_{n+1} &< \frac{A}{n^2} + \left(1 - \frac{B}{n}\right) \frac{C/n}{1+C/n} \\ &= \frac{C + (A - BC + AC/n)/n}{n+C}. \end{aligned}$$

If $C > 0$ is large enough, the expression in parentheses is negative (for large n), and we obtain $\lambda_{n+1} < C/(n+C) < C/(n+1)$, thus completing the induction.

Next we consider the turning period of the corner series. We just proved that $\lambda_{N_1} \asymp 1/N_1 \asymp 1/N$, and we noted in the previous section that $\tau_{N_1} \asymp 1/N^2$, hence $\mathcal{B}^+_{N_1} = \lambda_{N_1}/\tau_{N_1} \asymp N$. Then we can use the recursive formula

$$\mathcal{B}^+_{n+1} = \frac{2}{\sin \gamma_{n+1}} + \frac{\mathcal{B}^+_n}{1 + \tau_n \mathcal{B}^+_n},$$

see (4.7), to estimate $\mathcal{B}^+_n$ for $n \geq N_1$. Since

$$2 < \frac{2}{\sin \gamma_{n+1}} < \frac{2}{\sin \bar{\gamma}} =: G < \infty$$

for all $n \in (N_1, N_3)$, we have $\mathcal{B}_{n+1}^+ \le G + \mathcal{B}_n^+$, thus $\mathcal{B}_n^+ \le \mathcal{B}_{N_1} + NG \asymp N$ for $N_1 \le n \le N_3$. To get a lower bound on $\mathcal{B}_n^+$ recall that $\tau_n \le D/N^2$ for some $D > 0$. Assuming that $\mathcal{B}_n > dN$ for some small $d > 0$ we obtain

$$\mathcal{B}_{n+1}^+ \ge 2 + \frac{dN}{1 + (D/N^2)(dN)} \ge dN$$

for large N. Therefore, $\mathcal{B}_n^+ \asymp N$ and $\lambda_n = \tau_n \mathcal{B}_n^+ \asymp 1/N$ for $N_1 \le n \le N_3$.

During the exiting period, we use the 'countdown' index $m = N + 1 - n$ (see Remark 3.3), so that (4.11) takes form

$$\lambda_{m-1} = \frac{2\tau_{m-1}}{\sin \gamma_{m-1}} + \frac{\tau_{m-1}}{\tau_m} \frac{\lambda_m}{1 + \lambda_m}.$$

Also, all the asymptotic formulas obtained in the previous section for the entering period remain valid for the exiting period if one replaces n by m; in particular,

$$\frac{a}{m^2} < \frac{2\tau_{m-1}}{\sin \gamma_{m-1}} < \frac{A}{m^2} \quad \text{and} \quad 1 + \frac{b}{m} < \frac{\tau_{m-1}}{\tau_m} < 1 + \frac{B}{m}$$

for some constants $0 < a < A < \infty$ and $0 < b < B < \infty$ and all $m \ge 3$. Next we use the 'backward' induction on m, going down from $m = N_3$ to $m = 1$. Assuming that $\lambda_m > c/m$ we get

$$\begin{aligned}\lambda_{m-1} &> \frac{a}{m^2} + \left(1 + \frac{b}{m}\right) \frac{c/m}{1 + c/m} \\ &= \frac{c + [a + bc - c - c^2 + (ac - a - bc - ac/m)/m]/(m + c)}{m - 1}.\end{aligned}$$

If $c > 0$ is small enough, the expression in the brackets is positive (for large m), and we obtain $\lambda_{m-1} > c/(m-1)$, thus completing the induction. Assuming that $\lambda_m < C/m$ we get

$$\begin{aligned}\lambda_{m-1} &< \frac{A}{m^2} + \left(1 + \frac{B}{m}\right) \frac{C/m}{1 + C/m} \\ &= \frac{C + [A + BC - C - C^2 + (AC - A - BC - AC/m)/m]/(m + C)}{m - 1}.\end{aligned}$$

If $C > 0$ is large enough, the expression in the brackets is negative (for large m), and we obtain $\lambda_{m-1} < C/(m-1)$, thus completing the induction. The lemma is proved. $\square$

Remark 4.3. *Observe that during the exiting period $\lambda_m \asymp 1/m$ and $\tau_m \asymp m^{-4/3}N^{-2/3}$, cf. (3.32), hence $\mathcal{B}_m^+ = \lambda_m/\tau_m \asymp m^{1/3}N^{2/3}$ for all $m = 2, \dots, N - N_3$. The case $m = 1$ (i.e. $n = N$) is not included in our estimates, because it is the last collision in the corner series, so that $\tau_N \asymp 1$, which affects λ_N. However, for points $x \in E_N$ satisfying (4.8) we can still use (4.7), which gives us*

$$\mathcal{B}_N^+ \asymp \mathcal{B}_{N-1}^+ \asymp N^{2/3}.$$

Lemma 4.2 implies that $\sum_{n=1}^{N-1} \lambda_n^2 = \mathcal{O}(1)$, i.e. this sum is bounded uniformly in N. Hence for any $1 \le N' < N'' \le N$ we have

$$\prod_{n=N'}^{N''-1} (1+\lambda_n) = \exp\left[\sum_{n=N'}^{N''-1} \ln(1+\lambda_n)\right] \asymp \exp\left[\sum_{n=N'}^{N''-1} \lambda_n\right]. \tag{4.12}$$

In particular, during the turning period, we have $\sum_{n=N_1-1}^{N_3} \lambda_n \asymp 1$, hence the expansion is insignificant (it is uniformly bounded in N).

Next we estimate the expansion during the entering period.

Lemma 4.4. *For all $x \in E_N$ satisfying (4.8) we have $\prod_{n=1}^{N_1}(1+\lambda_n) \asymp N^{1/3}$.*

Proof. In view of (4.12), this is equivalent to $\sum_{n=1}^{N_1} \lambda_n = \frac{1}{3}\ln N_1 + \Delta_N$, where $\Delta_N = \mathcal{O}(1)$. It is enough to show that

$$\lambda_n = \frac{1}{3n} + \chi_n, \quad \text{where} \quad \sum_{n=1}^{N_1} \chi_n = \mathcal{O}(1). \tag{4.13}$$

The recursive formula (4.11) can be rewritten as

$$\lambda_{n+1} = \frac{2}{9n^2} + a_n + \left(1 - \frac{4}{3n} + b_n\right)\frac{\lambda_n}{1+\lambda_n}, \tag{4.14}$$

where, due to (3.33),

$$a_n = \mathcal{O}\Big(\frac{\ln n}{n^3} + \frac{\gamma_n^2}{n^2} + \frac{\Gamma_n}{n^3}\Big)$$

and, due to (3.34),

$$b_n = \mathcal{O}\Big(\frac{\ln n}{n^2} + \frac{\gamma_n^2}{n} + \frac{\Gamma_n}{n^2}\Big)$$

Note that $|a_n| \le c/n^2$ and $|b_n| \le c/n$ for some small $c > 0$; in fact $c > 0$ can be made arbitrarily small by choosing sufficiently small $\bar{\gamma} > 0$. To verify (4.13) it is convenient to change variable as

$$\lambda_n = \frac{1 + Z_n}{3n}. \tag{4.15}$$

We substitute (4.15) into (4.14) and obtain by direct calculation

$$Z_{n+1} = R_n + Z_n\Big[1 - \frac{1}{n} + b_n + \mathcal{O}\Big(\frac{1}{n^2}\Big) - Z_n\Big(\frac{1}{3n} + \mathcal{O}\Big(\frac{1}{n^2}\Big)\Big) + \mathcal{O}\Big(\frac{Z_n^2}{n^2}\Big)\Big],$$

where

$$\begin{aligned} R_n &= 3na_n + b_n + \mathcal{O}(1/n^2) \\ &= \mathcal{O}\Big(\frac{\ln n}{n^2} + \frac{\gamma_n^2}{n} + \frac{\Gamma_n}{n^2}\Big). \end{aligned} \tag{4.16}$$

Observe that $Z_n > -1$ because $\lambda_n > 0$. It is clear that Z_n gets closer to zero as n grows, but we need more precise asymptotics. If we fix a small $\delta > 0$, then for large enough n we have

$$|Z_{n+1}| \le |R_n| + |Z_n|\Big(1 - \frac{\delta}{n}\Big).$$

Without affecting the asymptotic behavior of Z_n's we can assume that the above bound is valid for all n. Using it recurrently we obtain

$$\begin{aligned} |Z_n| &\le |R_n| + \sum_{k=1}^{n-1} |R_k| \prod_{i=k}^{n-1} \Big(1 - \frac{\delta}{i+1}\Big) \\ &\le \text{ const} \sum_{k=1}^{n} |R_k|\, e^{-\sum_{i=k}^{n} \delta/(i+1)} \\ &\le \text{ const} \sum_{k=1}^{n} |R_k| (k/n)^{\delta}. \end{aligned}$$

Now we are ready to verify (4.13):

$$\begin{aligned}\sum_{n=1}^{N_1} |\chi_n| &\le \text{ const} \sum_{n=1}^{N_1} |Z_n|/n \\ &\le \text{ const} \sum_{n=1}^{N_1} \sum_{k=1}^{n} |R_k| k^\delta / n^{1+\delta} \\ &\le \text{ const} \sum_{k=1}^{N_1} |R_k| \sum_{n=k}^{N_1} k^\delta / n^{1+\delta} \\ &\le \text{ const} \sum_{k=1}^{N_1} |R_k|.\end{aligned}$$

Due to (4.16), the last sum is bounded uniformly in N. The lemma is proved. $\square$

It remains to estimate the expansion during the exiting period:

Lemma 4.5. *For all $x \in E_N$ satisfying (4.8) we have $\prod_{n=N_3}^{N-1}(1+\lambda_n) \asymp N^{2/3}$.*

Proof. Our argument follows the lines of the previous proof and we again use the countdown index $m = N - n + 1$. In view of (4.12), the lemma is equivalent to $\sum_{m=2}^{N-N_3} \lambda_m = \frac{2}{3} \ln(N - N_3) + \Delta_N$, where $\Delta_N = \mathcal{O}(1)$. It is enough to show that

$$\lambda_m = \frac{2}{3m} + \chi_m, \quad \text{where} \quad \sum_{m=2}^{N-N_3} \chi_m = \mathcal{O}(1) \tag{4.17}$$

The recursive formula (4.11) now takes form

$$\lambda_{m-1} = \frac{2}{9m^2} + a_m + \left(1 + \frac{4}{3m} + b_m\right) \frac{\lambda_m}{1 + \lambda_m}, \tag{4.18}$$

where, due to (3.33),

$$a_m = \mathcal{O}\Big(\frac{\ln m}{m^3} + \frac{\gamma_m^2}{m^2} + \frac{\Gamma_m}{m^3}\Big)$$

and, due to (3.34),

$$b_m = \mathcal{O}\Big(\frac{\ln m}{m^2} + \frac{\gamma_m^2}{m} + \frac{\Gamma_m}{m^2}\Big).$$

Note that $|a_m| \le c/m^2$ and $|b_m| \le c/m$ for some small $c > 0$ (and c can be made arbitrarily small by choosing sufficiently small $\bar{\gamma}$). To verify (4.17) it is convenient to change variable as

$$\lambda_m = 2\,\frac{1+Z_m}{3m}. \tag{4.19}$$

We substitute (4.19) into (4.18) and obtain by direct calculation

$$Z_{m-1} = R_m + Z_m\Big[1 - \frac{1}{m} + b_m + \mathcal{O}\Big(\frac{1}{m^2}\Big) - Z_m\Big(\frac{1}{3m} + \mathcal{O}\Big(\frac{1}{m^2}\Big)\Big) + \mathcal{O}\Big(\frac{Z_m^2}{m^2}\Big)\Big],$$

where

$$\begin{aligned} R_m &= 3ma_m + b_m + \mathcal{O}(1/m^2) \\ &= \mathcal{O}\Big(\frac{\ln m}{m^2} + \frac{\gamma_m^2}{m} + \frac{\Gamma_m}{m^2}\Big). \end{aligned} \tag{4.20}$$

If we fix a small $\delta > 0$, then for large enough m we have

$$|Z_{m-1}| \le |R_m| + |Z_m|\Big(1 - \frac{\delta}{m}\Big).$$

Without affecting the asymptotic behavior of Z_m's we can assume that the above bound is valid for all $m \ge 3$. Using it recurrently we obtain

$$\begin{aligned} |Z_m| &\le \sum_{k=m}^{N-N_3} |R_k| \prod_{i=m}^{k} \Big(1 - \frac{\delta}{i}\Big) \\ &\le \text{ const } \sum_{k=m}^{N-N_3} |R_k|\, e^{-\sum_{i=m}^{k} \delta/i} \\ &\le \text{ const } \sum_{k=m}^{N-N_3} |R_k| (m/k)^{\delta}. \end{aligned}$$

Now we are ready to verify (4.17):

$$\begin{aligned}\sum_{m=2}^{N-N_3}|\chi_m| &\leq \text{const}\sum_{m=2}^{N-N_3}|Z_m|/m\\ &\leq \text{const}\sum_{m=2}^{N-N_3}\sum_{k=m}^{N-N_3}|R_k|m^{\delta-1}/k^{\delta}\\ &\leq \text{const}\sum_{k=2}^{N-N_3}|R_k|\sum_{m=2}^{k}m^{\delta-1}/k^{\delta}\\ &\leq \text{const}\sum_{k=2}^{N}|R_k|.\end{aligned}$$

Due to (4.20), the last sum is bounded uniformly in N. The lemma is proved. □

After the last collision, the particle leaves the cusp and flies back to the vicinity of the point $D \in \partial\mathcal{D}$. According to Remark 4.3, $\mathcal{B}_N^+ \asymp N^{2/3}$ and $\tau_N \asymp 1$, hence unstable vectors are additionally expanded by $1 + \tau_N\mathcal{B}_N^+ \asymp N^{2/3}$. Thus the total expansion factor for unstable vectors $dx \in \mathcal{T}_x\mathcal{M}$ is

$$\frac{\|D_x\mathcal{F}^{N+1}(dx)\|_p}{\|dx\|_p} \asymp N^{1/3} \times N^{2/3} \times N^{2/3} = N^{5/3}$$

for all $x \in E_N$ satisfying (4.8).

For points $x \in E_N$ where γ_1 fails to satisfy (4.8), the expansion between the first and second collisions is

$$\frac{\|D_{x_1}\mathcal{F}(dx_1)\|_p}{\|dx_1\|_p} = 1 + \tau_1\mathcal{B}_1^+ \asymp 1 + \frac{N^{-2/3}}{\cos\varphi_1},$$

which accounts for the first extra factor in (4.5). For points $x \in E_N$ where γ_N fails to satisfy (4.8), the expansion between the last collision at x_N and return to $\hat{\mathcal{M}}$ (near D) is

$$\begin{aligned}\frac{\|D_{x_N}\mathcal{F}(dx_N)\|_p}{\|dx_N\|_p} &= 1 + \tau_N\mathcal{B}_N^+ \asymp \mathcal{B}_N^+\\ &= 2/\cos\varphi_N + \mathcal{B}_N^-\\ &\asymp [\cos\varphi_N]^{-1} + N^{2/3}\\ &\asymp N^{2/3}\left(1 + \frac{N^{-2/3}}{\cos\varphi_N}\right),\end{aligned}$$

which accounts for the second extra factor in (4.5).

This completes the proof of Proposition 4.1. □

5 Cell structure

Here we use the results of the previous two sections to analyze the sets E_N, which consist of points whose trajectories go down a cusp and experience there a corner series of exactly N collisions.

We will use standard facts of the theory of dispersing billiards [BSC90, BSC91, C99, CM06]. For example, the domains E_N are bounded by singularity curves of the map $\hat{\mathcal{F}}$ (which are singularity curves for the maps $\mathcal{F}^i$, $i = 1, \dots, N$, with $N = R(x)$); the latter are smooth compact curves whose slope in the $r\varphi$ coordinates is negative and bounded away from zero and infinity, i.e.

$$-\infty < C_1 \leq d\varphi/dr \leq C_2 < 0$$

for some constants C_1, C_2. The images $F_N = \hat{\mathcal{F}}(E_N)$ are domains bounded by singularity curves of the map $\hat{\mathcal{F}}^{-1}$, which are smooth compact curves with *positive* slope. Moreover, due to the time-reversibility of the billiard dynamics, we have a handy symmetry: a point (r, φ) belongs in E_N if and only if $(r, -\varphi) \in F_N$, hence F_N is obtained by reflecting E_N across the line $\varphi = 0$. More generally, a point (r, φ) is a singularity point for the map $\hat{\mathcal{F}}$ if and only if $(r, -\varphi)$ is a singularity point for its inverse $\hat{\mathcal{F}}^{-1}$.

For simplicity, we again consider the three-arc billiard table shown on Fig. 1. There are three identical spots in $\hat{\mathcal{M}}$ from which trajectories depart into cusps: their footpoints must be near D, E, or F (opposite to the cusps A, B, and C, respectively), and the velocities of such trajectories must be nearly orthogonal to $\partial\mathcal{D}$.

Consider one such spot, near the point $x_D = (r_D, 0)$, where r_D denotes the r-coordinate of D. A simple geometric inspection shows that x_D itself belongs to a singularity curve, call it S_0 (see the thick black line on Fig. 5, going from 'northwest' to 'southeast'); it is made by trajectories whose very first collision in the cusp is grazing. One can easily check that the slope of the curve S_0 at x_D is $d\varphi/dr = -(3 + \sqrt{3})/2$.

The domain E_N (more precisely, its part near x_D) is a union of two 'bent' strips (colored grey on Fig. 5), we denote them by E'_N and E''_N. Each strip is bounded by an 'outer' curve, call it S_{N-1}, and an 'inner' curve, call it S_N (as well as two short segments of S_0). The curves S_N and S_{N-1} bounding

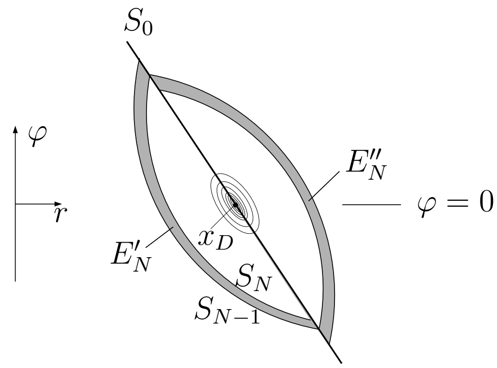

Figure 5: The domain E_N near the point x_D.

$E_N = E'_N \cup E''_N$ terminate on S_0. The domains E_N, $N > K_0$, make a 'nested' structure and shrink to x_D as $N \to \infty$ (they are schematically shown by concentric ovals on Fig. 5). The curves S_N separating the domain E_N from E_{N+1} are made by trajectories whose *last* collision in the corner series is grazing.

Why do we have two parts (two strips) of the domain E_N, one above S_0 and the other below S_0? It is because the first collision of a corner series of length N may occur on either of the two arcs making the cusp (left or right), and each strip contains points coming down onto one of these arcs (the strip E''_N above S_0 hits the left arc first, the strip E'_N below S_0 hits the right arc first).

To determine the dimensions of the strips E'_N and E''_N observe that their extreme points (lying the curve S_0 and located farthest from the central point x_D) are made by trajectories whose very first collision in the cusp is grazing, see the solid lines on Fig. 6. Since the point of the first collision in the cusp is the distance $\asymp N^{-2/3}$ from the vertex A, according to (3.2), we conclude that the trajectory originates the distance $\asymp N^{-2/3}$ from the point D. Thus the diameter of E'_N and E''_N (i.e. the 'length' of these strips) is $\asymp N^{-2/3}$.

The middle parts of E'_N and E''_N (closest to the point x_D) are made by trajectories starting out at angles $|\varphi| \asymp N^{-4/3}$, see the dashed lines on Fig. 6, thus $\text{dist}(E_N, x_D) \asymp N^{-4/3}$. This suggests that the width of the strips making E_N is $\asymp N^{-7/3}$, but we will deduce this estimate from the results of the previous section.

Due to the aforementioned symmetry, the image $F_N = \hat{\mathcal{F}}(E_N)$ is congru-

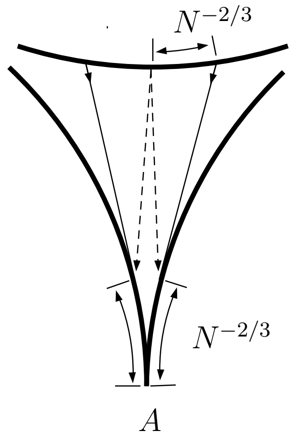

Figure 6: Extremal trajectories in E_N.

ent to E_N itself, in particular it consists of two strips, F'_N and F''_N of length $\asymp N^{-2/3}$, see Fig. 7. Without loss of generality we suppose that $\hat{\mathcal{F}}(E'_N) = F'_N$ (this is the case when N is even, otherwise we have $\hat{\mathcal{F}}(E'_N) = F''_N$). If $W \subset E'_N$ is an unstable curve stretching across E'_N (from S_N to S_{N-1}), see Fig. 7, then its image $\hat{\mathcal{F}}(W)$ will stretch 'from top to bottom' of F'_N, so its length will be $|\hat{\mathcal{F}}(W)| \asymp N^{-2/3}$. Due to Proposition 4.1, we obtain $|W| \asymp N^{-2/3}/N^{5/3} = N^{-7/3}$, which is exactly the width of the strip E'_N.

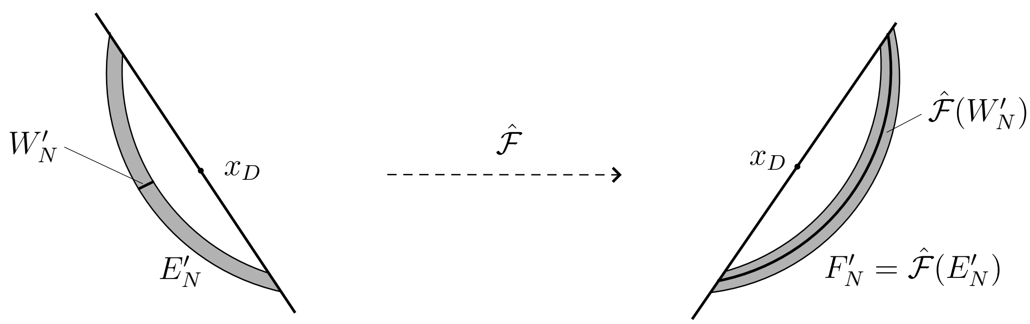

Figure 7: An unstable curve $W'_N \subset E'_N$ and its image $\hat{\mathcal{F}}(W) \subset F'_N$.

It is now clear that

$$\hat{\mu}(E_N) \asymp \mu(E_N) \asymp N^{-2/3} \times N^{-7/3} = N^{-3},$$

thus

$$\hat{\mu}(x \in \hat{\mathcal{M}}\colon R(x) > N) \asymp N^{-2},$$

hence (2.3) holds with $a = 2$. This completes the proof of Theorem 1.1, except we have not yet verified all the conditions of Theorem 2.1: it remains to prove the following:

Proposition 5.1. *The map $\hat{\mathcal{F}}\colon \hat{\mathcal{M}} \to \hat{\mathcal{M}}$ has exponential decay of correlations.*

Proof. According to [CZ05a], it is enough to verify a set of standard conditions. These include several conditions of technical nature (distortion bounds, absolute continuity, curvature bounds for singularity lines, etc.), which for dispersing billiards without cusps have been verified in other papers [BSC91, C99] and in our book [CM06], and their verification for billiards with cusps only require minor changes. We only deal with the main condition on the expansion of unstable curves here,

Let $\mathcal{S}$ denote the singularity set for the map $\hat{\mathcal{F}}$. These include the points where $\hat{\mathcal{F}}$ is discontinuous as well as the preimages of the boundaries of homogeneity strips, see below. For any unstable curve $W \subset \hat{\mathcal{M}}$ denote by W_i, $i \geq 1$, the connected components of $W \setminus \mathcal{S}$. For every i let Λ_i be the minimal factor of expansion of W_i under $\hat{\mathcal{F}}$ (due to the distortion bounds, this factor does not vary much over W_i). Then the expansion condition to be verified is

$$\liminf_{\delta \to 0} \sup_{W\colon |W| < \delta} \sum_i \Lambda_i^{-1} < 1, \tag{5.1}$$

where the supremum is taken over unstable curves W of length $|W| < \delta$.

Let $\mathcal{S}_{1,d}$ denote the set where the map $\hat{\mathcal{F}}$ is discontinuous. In the vicinity of x_d, the set $\mathcal{S}_{1,d}$ is the union of the curve S_0 and all the curves S_N, $N \geq K_0$.

Any unstable curve $W \subset \hat{\mathcal{M}}$ is increasing in the $r\varphi$ coordinates, hence it can only intersect any given discontinuity curve S_i once. But it may intersect infinitely many (or all!) of them, hence $W \setminus \mathcal{S}_{1,d}$ may have countably many connected components. Each component lies in one strip of E_N for some $N \geq K_0$, and we denote them by $W'_N = W \cap E'_N$ and $W''_N = W \cap E''_N$.

Consider an arbitrary component W'_N, $N \geq K_0$. It must be further subdivided into finitely or countably many 'homogeneous' subcomponents in the following way. For every $i = 1, \dots, N$, if the image $\mathcal{F}^i(W'_N)$ crosses the boundary of a homogeneity strip (defined below) at a point $y \in \mathcal{F}^i(W'_N)$, then the curve W'_N must be subdivided at the point $\mathcal{F}^{-i}(y)$.

Homogeneity strips were introduced in [BSC91] for a better control over distortions, see also [CM06, Chapter 5]. We fix a large constant $k_0 \gg 1$ and for each $k \geq k_0$ define two strips $\mathbb{H}_{\pm k} \subset \mathcal{M}$ by

$$\mathbb{H}_k = \{(r, \varphi) \colon \pi/2 - k^{-2} < \varphi < \pi/2 - (k+1)^{-2}\}$$

and

$$\mathbb{H}_{-k} = \{(r, \varphi) \colon -\pi/2 + (k+1)^{-2} < \varphi < -\pi/2 + k^{-2}\}.$$

Now $\mathcal{M}$ is divided into homogeneity strips $\mathbb{H}_k$ bounded by the lines

$$\mathbb{S}_{\pm k} = \{(r, \varphi) \colon \pm\varphi = \pi/2 - k^{-2}\}$$

for $|k| \geq k_0$; these are countably many horizontal lines on the $r\varphi$ coordinate plane accumulating near the natural boundary $|\varphi| = \pi/2$, see Fig. 8.

Consider the domains $G^i = \mathcal{F}^i(E'_N)$ for $i = 1, \dots, N$. A direct geometric inspection shows that the very first one, G^1, is a strip adjacent to the boundary $\varphi = -\pi/2$, see Fig. 8; its length in the 'negative' (northwest–southeast) direction is $\asymp N^{-2/3}$, and its width in the 'positive' (northeast–southwest) direction is $\asymp N^{-5/3}$ (this follows from our estimates on the size of E'_N and our analysis of expansion of unstable curves in Section 4). It crosses infinitely many lines $\mathbb{S}_{-k}$, $k \geq k_N$, where $k_N^{-2} \asymp N^{-2/3}$, hence $k_N \asymp N^{1/3}$. Further images G^i, $i \geq 2$, move away from the boundary $|\varphi| = \pi/2$, see Fig. 8, thus they can only cross $2k_N \asymp N^{1/3}$ lines $\mathbb{S}_{\pm k}$, $k \leq k_N$.

When i approaches N, this picture is repeated in the reverse order: the domains G^i, $N/2 \leq i \leq N-1$, intersect finitely many lines $\mathbb{S}_{\pm k}$, $k \leq k_N$, and the last domain G^N intersects countably many lines $\mathbb{S}_{-k}$, $k \geq k_N$.

Since any unstable curve has a positive slope, $d\varphi/dr > 0$, it may only intersect each line $\mathbb{S}_k$ once. Thus every line $\mathbb{S}_k$ can only induce one point in the curve W'_N where the latter must be subdivided. Most important are the intersections of $\mathbb{S}_{-k}$, $k \geq k_N$, with the very first image $\mathcal{F}(W'_N)$ and the very last image $\mathcal{F}^N(W'_N)$. They induce a partition of W'_N into countably many subcomponents that we denote by

$$W'_{N,k,m} = W'_N \cap \mathcal{F}^{-1}(\mathbb{H}_{-k}) \cap \mathcal{F}^{-N}(\mathbb{H}_{-m}), \tag{5.2}$$

$k, m \geq k_N$. Observe that $\cos\varphi \asymp k^{-2}$ in the strips $\mathbb{H}_{\pm k}$. Thus, according to (4.5), the map $\hat{\mathcal{F}}$ expands the subcomponent $W'_{N,k,m}$ by a factor of

$$\Lambda_{N,k,m} \asymp N^{5/3}(1 + k^2 N^{-2/3})(1 + m^2 N^{-2/3}).$$

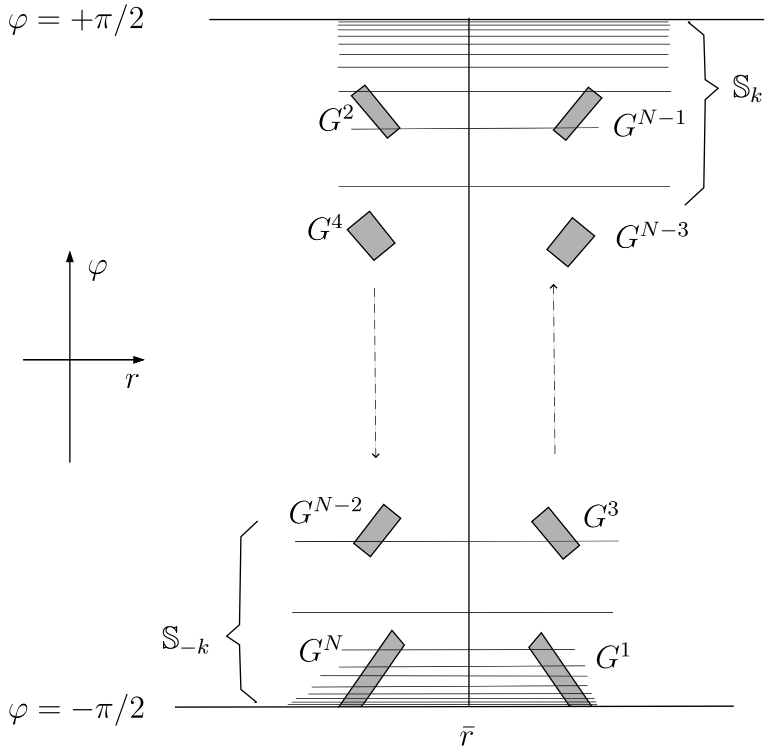

Figure 8: The images $G^i = \mathcal{F}^i(E'_N)$ and the lines $\mathbb{S}_{\pm k}$. The vertical line corresponds to $\bar{r} = r_A$, the r-coordinate of the vertex A.

We now estimate from above the following sum:

$$\sum_{(k,m)\in Z_N} \Lambda^{-1}_{N,k,m} \asymp N^{-5/3} \sum_{(k,m)\in Z_N} (1 + k^2 N^{-2/3})^{-1}(1 + m^2 N^{-2/3})^{-1}, \tag{5.3}$$

where Z_N is the set of pairs (k, m) for which the intersection (5.2) is not empty. Observe that if the curve W'_N is traversed from one end to the other, then both indices k and m change monotonically.

In the case treated here (which is shown on Figs. 7 and 8) both indices increase or both decrease depending on the direction in which the curve W'_N is traversed. Thus, if we join each pair of neighboring points of the set $Z_N \subset \mathbb{R}^2$ by a unit segment, we will get a monotonically increasing polygonal line in the quadrant $\{k \geq k_N, m \geq k_N\}$ starting at (k_N, k_N). For every $n \geq 2k_N$

there is at most one pair $(k, m) \in Z_N$ such that $k+m=n$. For a fixed value of $k+m=n$, by a simple application of Cauchy-Schwarz inequality we get

$$(1+k^2N^{-2/3})(1+m^2N^{-2/3}) \geq N^{-2/3}n^2,$$

thus

$$\begin{aligned}\sum_{(k,m)\in Z_N} \Lambda^{-1}_{N,k,m} &\leq \text{const}\cdot N^{-5/3}\sum_{n=2k_N}^{\infty} N^{2/3}n^{-2}\\ &\asymp N^{-1}\int_{2k_N}^{\infty}\frac{dx}{x^2}\\ &\asymp N^{-1}N^{-1/3} = N^{-4/3}.\end{aligned}$$

In other cases (say, for $W''_N = W \cap E''_N$) it might happen that, as the curve W'_N is traversed from one end to the other, then the indices k and m change in the opposite way: k increases and m decreases (or vice versa). Then, if we join each pair of neighboring points of the set $Z_N \subset \mathbb{R}^2$ by a unit segment, we will get a monotonically *decreasing* polygonal line in the quadrant $\{k \geq k_N, m \geq k_N\}$. For every $n \in \mathbb{Z}$ there will be at most one pair $(k, m) \in Z_N$ such that $k-m=n$. For a fixed value of $k-m=n$, we obviously have

$$(1+k^2N^{-2/3})(1+m^2N^{-2/3}) \geq (1+k_N^2N^{-2/3})(1+(k_N+|n|)^2N^{-2/3})$$

thus

$$\begin{aligned}\sum_{(k,m)\in Z_N} \Lambda^{-1}_{N,k,m} &\leq \frac{\text{const}\cdot N^{-5/3}}{1+k_N^2N^{-2/3}}\sum_{n=k_N}^{\infty}\frac{1}{1+n^2N^{-2/3}}\\ &\asymp N^{-5/3}\int_{k_N}^{\infty}\frac{dx}{1+N^{-2/3}x^2}\\ &\asymp N^{-5/3}N^{1/3} = N^{-4/3}.\end{aligned}$$

which is the same upper bound as in the previous case.

Next, we need to add intersections of the lines $\mathbb{S}_{\pm k}$, $k \leq k_N$, with the intermediate images $\mathcal{F}^i(W'_N)$, $2 \leq i \leq N-1$. These contribute at most $2k_N$ additional points of intersection, i.e. at most $2k_N$ additional subcomponents in W'_N. The minimal expansion factor of the map $\hat{\mathcal{F}}$ along the curve W'_N is $\asymp N^{-5/3}$, thus additional $2k_N$ subcomponents will contribute the amount

$\leq$ const $\cdot\, k_N\, N^{-5/3} \asymp N^{-4/3}$, which is of the same order of magnitude as the sum (5.3).

Thus for every component $W_N' = W \cap E_N'$ of the original unstable curve W the sum of the reciprocals of the minimal expansion factors over all its subcomponents is bounded above by const $\cdot\, N^{-4/3}$. It remains to sum up over $N \geq K_0$:

$$\text{const} \sum_{N=K_0}^{\infty} N^{-4/3} \leq \text{const} \cdot K_0^{-1/3} < 1,$$

which is true if K_0 is chosen large enough. This proves (5.1) for unstable curves going through long corner series. For all the other unstable curves the dynamics is not different from that in 'regular' dispersing billiards (without cusps), where (5.1) has been verified in [Y98, C99], see also [CM06, Chapter 5]. Proposition 5.1 is proved. □

This completes the proof of Theorem 1.1 for the special three-arc table shown on Fig. 1. □

6 General case

In the previous sections we restricted our analysis to the three-arc billiard table with cusps introduced by Machta [Mac83] and shown on Fig. 1. This made our calculations relatively simple and geometrically transparent. Here we outline changes necessary for proving Theorem 1.1 in the general case.

Let a cusp be made by two boundary components $\Theta_1, \Theta_2 \subset \partial\mathcal{D}$. Choose the coordinate system as shown on Fig. 9, then the equations of Θ_1 and Θ_2 are, respectively, $y = f_1(x)$ and $y = -f_2(x)$, where f_i are convex C^3 functions, $f_i(x) > 0$ for $x > 0$, and $f_i(0) = f_i'(0) = 0$ for $i = 1, 2$. We will use Taylor polynomial for the functions f_i and their derivatives:

$$f_i(x) = \tfrac{1}{2} a_i x^2 + \mathcal{O}(x^3), \qquad f_i'(x) = a_i x + \mathcal{O}(x^2), \qquad f_i''(x) = a_i + \mathcal{O}(x),$$

where $a_i = f_i''(0)$. Since the curvature of the boundary of dispersing billiards must not vanish, we have $a_i > 0$ for $i = 1, 2$. For the particular three-arc table analyzed earlier, $f_1(x) = f_2(x) = 1 - \sqrt{1 - x^2}$.

Consider a billiard trajectory entering the cusp and making a long series of N reflections there. We denote reflection points by (x_n, y_n), where $y_n = f_1(x_n)$ or $y_n = -f_2(x_n)$ depending on which side of the cusp the reflection

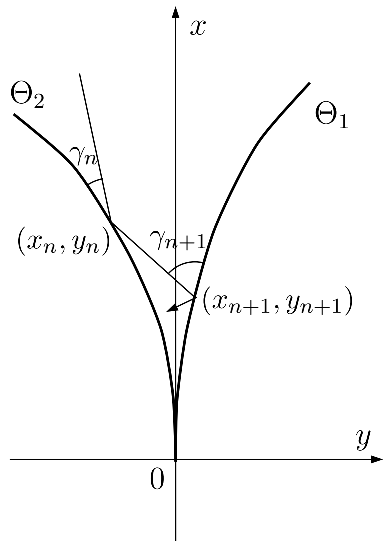

Figure 9: A cusp made by two curves, Θ_1 and Θ_2.

occurs. As in Section 3, we use φ_n and $\gamma_n = \pi/2 - |\varphi_n|$ for the angle of reflection, but do not use α_n any more (its role will be played by x_n). Generally, we will use the same symbols as in Sections 3–4 (to make our presentations here and there comparable), but some symbols will now have a slightly different meaning.

As in Section 3, we denote by N_2 the deepest collision (closets to the vertex of the cusp). Clearly, the collisions occur alternatively from the two sides of the cusp, they go down the cusp monotonically, and then return back up monotonically as well:

$$x_1 > x_2 > \cdots > x_{N_2} \leq x_{N_2+1} < x_{N_2+2} < \cdots < x_N$$

(possibly, two deepest collisions have equal x-coordinates).

Lemma 3.1 partially extends to the general case. Namely, let $x_m = x_{N_2}$ be the deepest collision, and assume without loss of generality that $x_{m+1} \geq x_{m-1}$. Then

$$x_{m+i} \geq x_{m-i} \qquad \text{and} \qquad \gamma_{m+i} \leq \gamma_{m-i}$$

for all $i = 1, 2, \ldots$, as long as both collisions remain in the corner series. This implies that $|N_2 - N/2| = \mathcal{O}(1)$.

As in Section 3, we fix a small $\bar{\gamma} > 0$ and introduce N_1 and N_3 accordingly, this divides the corner series into three periods: entering, turning, and exiting ones.

Our first task is to extend Proposition 3.2 to the general case. Consider two successive reflections at points (x_n, y_n) and (x_{n+1}, y_{n+1}) with angles γ_n and γ_{n+1}. Without loss of generality, let $y_n = -f_2(x_n)$, hence $y_{n+1} = f_1(x_{n+1})$. A direct geometric inspection shows that

$$\gamma_{n+1} = \gamma_n + \tan^{-1} f_2'(x_n) + \tan^{-1} f_1'(x_{n+1}) \tag{6.1}$$

and

$$x_{n+1} = x_n - \frac{f_2(x_n) + f_1(x_{n+1})}{\tan\bigl[\gamma_n + \tan^{-1} f_2'(x_n)\bigr]}, \tag{6.2}$$

as long as the trajectory goes down the cusp, i.e. $n < N_2$. Equations (6.1)–(6.2) are analogues of the simpler relations (3.6)–(3.7) used in Section 3. All the arguments of that section will carry over to the general case by way of Taylor expansion of all the functions involved in (6.1)–(6.2). We only outline main steps, the reader should have no trouble filling missing details. First, (6.1) gives

$$\gamma_{n+1} = \gamma_n + a_2 x_n + a_1 x_{n+1} + \mathcal{O}(x_n^2),$$

and adding these up for $1 \le n < N_2$ gives

$$x_1 + \cdots + x_{N_2} = \mathcal{O}(1)$$

(remember that $a_1, a_2 > 0$), which is an analogue of (3.9).

Next we introduce variables:

$$u_n = \frac{x_{n+1}}{x_n} \quad \text{and} \quad w_n = \frac{\gamma_n}{x_n}.$$

Due to (6.1), we obtain an analogue of (3.12):

$$w_{n+1} = a_1 + \frac{w_n + a_2 + \mathcal{O}(x_n)}{u_n} \tag{6.3}$$

and since $u_n \le 1$ it follows that $w_n \ge 2\bar{a}n + \mathcal{O}(1)$, where $\bar{a} = (a_1 + a_2)/2$.

Using (6.2) and the obvious $\tan x > x$ gives

$$u_n > 1 - \frac{\bar{a}}{w_n + a_2}\bigl[1 + \mathcal{O}(x_n)\bigr]. \tag{6.4}$$

Combining (6.3) with (6.4) gives

$$\begin{aligned} w_{n+1} &< a_1 + \big(w_n + a_2 + \mathcal{O}(x_n)\big)\left(1 + \frac{\bar a}{w_n + a_2}\big[1 + \mathcal{O}(x_n)\big] + \mathcal{O}(w_n^{-2})\right) \\ &= w_n + 3\bar a + \mathcal{O}(x_n) + \mathcal{O}(w_n^{-1}), \end{aligned}$$

therefore $w_n \le 3\bar a n + \mathcal{O}(\ln n)$. So we obtain $w_n \asymp n$, hence $\gamma_n \asymp n\alpha_n$, in particular $\alpha_{N_2} \asymp 1/N_2$.

A more precise asymptotical formula follows from (6.2):

$$u_n = 1 - \frac{a_2 + a_1 u_n^2 + \mathcal{O}(x_n + \gamma_n^2)}{2(w_n + a_2)}, \tag{6.5}$$

and combining (6.3) with (6.5) gives

$$\begin{aligned} w_{n+1} &= w_n + a_1 + a_2 + \frac{a_2 + a_1 u_n^2}{2} + \mathcal{O}(x_n + \gamma_n^2 + n^{-1}) \\ &= w_n + 3\bar a + \mathcal{O}(x_n + \gamma_n^2 + n^{-1}), \end{aligned} \tag{6.6}$$

where we used the established fact $u_n = 1 - \mathcal{O}(n^{-1})$. Therefore

$$w_n = 3\bar a n + \mathcal{O}(\ln n + \Gamma_n),$$

where $\Gamma_n = \gamma_1^2 + \cdots + \gamma_n^2$, as in Section 3. It is easy to verify the relations (3.30). Next, (6.3) implies

$$\begin{aligned} u_n^{-1} &= \frac{w_{n+1} - a_1}{w_n + a_2}\left(1 + \mathcal{O}\Big(\frac{x_n}{n}\Big)\right) \\ &= 1 + \frac{1}{3n + \mathcal{O}(\ln n + \Gamma_n)} + \mathcal{O}\Big(\frac{x_n}{n} + \frac{\gamma_n^2}{n} + \frac{1}{n^2}\Big) \end{aligned}$$

Multiplying over n gives

$$x_1/x_n = u_1^{-1} \cdots u_{n-1}^{-1} \asymp n^{1/3},$$

hence $\gamma_n \asymp x_1 n^{2/3}$. In particular, $x_1 \asymp N_1^{-2/3}$ and $x_{N_1} \asymp 1/N_1$.

The analysis of the turning period is easily done as in Section 3 and gives $N_1 \asymp N$ and $x_{N_2} \asymp 1/N$. Note that $x_n = \mathcal{O}(1/n)$, hence the x_n's can be absorbed by $1/n$ in the previous formulas, and then we get exactly the same formulas (3.27), (3.28), and (3.29) as in Section 3, except we now have an extra factor of $\bar{a}$ in (3.27) and (3.28).

Next, the intercollision time (=distance) is

$$\begin{aligned}\tau_n &= \frac{f_2(x_n) + f_1(x_{n+1})}{\sin\bigl(\gamma_n + \tan^{-1} f_2'(x_n)\bigr)} \\ &= \frac{x_n}{2w_n} \frac{a_2 + a_1 u_n^2 + \mathcal{O}(x_n)}{1 + a_2 w_n^{-1} + \mathcal{O}(\gamma_n^2)} \\ &= x_n w_n^{-1}\bigl(\bar{a} + \mathcal{O}(n^{-1} + \gamma_n^2)\bigr) \\ &\asymp x_n/n \asymp n^{-4/3} N^{-2/3}.\end{aligned}$$

It follows that

$$\begin{aligned}\frac{\tau_n}{\sin\gamma_n} &= \frac{\bar{a}}{w_n^2}\bigl(1 + \mathcal{O}(n^{-1} + \gamma_n^2)\bigr) \\ &= \frac{1}{9\bar{a}n^2} + \mathcal{O}\Bigl(\frac{\ln n}{n^3} + \frac{\gamma_n^2}{n^2} + \frac{\Gamma_n}{n^3}\Bigr).\end{aligned} \tag{6.7}$$

Next we estimate

$$\frac{\tau_{n+1}}{\tau_n} = \frac{f_1(x_{n+1}) + f_2(x_{n+2})}{f_2(x_n) + f_1(x_{n+1})} \times \frac{\sin\bigl(\gamma_n + \tan^{-1} f_2'(x_n)\bigr)}{\sin\bigl(\gamma_{n+1} + \tan^{-1} f_1'(x_{n+1})\bigr)} =: F_n' \times F_n''.$$

First,

$$\begin{aligned}F_N' &= \frac{a_1 x_{n+1}^2 + a_2 x_{n+2}^2 + \mathcal{O}(x_n^3)}{a_2 x_n^2 + a_1 x_{n+1}^2 + \mathcal{O}(x_n^3)} \\ &= \frac{u_n^2(a_1 + a_2 u_{n+1}^2) + \mathcal{O}(x_n)}{a_2 + a_1 u_n^2 + \mathcal{O}(x_n)} \\ &= 1 - \frac{2+\Delta}{3n} + \mathcal{O}\Bigl(\frac{\ln n}{n^2} + \frac{\gamma_n^2}{n} + \frac{\Gamma_n}{n^2} + x_n\Bigr)\end{aligned}$$

where $\Delta = (a_2 - a_1)/\bar{a}$. Using the same argument as in Section 3 we get

$$\begin{aligned}
F_N'' &= 1 - \frac{\sin\bigl(\gamma_{n+1} + \tan^{-1} f_1'(x_{n+1})\bigr) - \sin\bigl(\gamma_n + \tan^{-1} f_2'(x_n)\bigr)}{\sin\bigl(\gamma_{n+1} + \tan^{-1} f_1'(x_{n+1})\bigr)} \\
&= 1 - \frac{\bigl[\gamma_{n+1} - \gamma_n + a_1 x_{n+1} - a_2 x_n + \mathcal{O}(x_n^2)\bigr]\,\bigl[1 + \mathcal{O}(\gamma_n^2)\bigr]}{x_n u_n (w_{n+1} + a_1) + \mathcal{O}(x_n^2 + \gamma_n^3)} \\
&= 1 - \frac{w_n(u_n - 1) + (3\bar{a} + a_1)u_n - a_2 + \mathcal{O}(n^{-1} + \gamma_n^2)}{u_n(w_{n+1} + a_1) + \mathcal{O}(x_n)} \Bigl(1 + \mathcal{O}(\gamma_n^2)\Bigr) \\
&= 1 - \frac{2 - \Delta}{3n} + \mathcal{O}\Bigl(\frac{\ln n}{n^2} + \frac{\gamma_n^2}{n} + \frac{\Gamma_n}{n^2}\Bigr).
\end{aligned}$$

Therefore,

$$\frac{\tau_{n+1}}{\tau_n} = 1 - \frac{4}{3n} + \mathcal{O}\Bigl(\frac{\ln n}{n^2} + \frac{\gamma_n^2}{n} + \frac{\Gamma_n}{n^2} + x_n\Bigr),$$

(note that Δ cancels out!). This is almost identical to (3.34); the extra term x_n will not cause trouble as $\sum x_n = \mathcal{O}(1)$. In summary, all the main formulas here are similar to those in Section 3, with a notable exception: an extra factor of $\bar{a}$ in the expressions for w_n and in (6.7).

The extension of the results of Section 4 to the general case is pretty straightforward, the only serious change involves the recursive formula (4.7) which now takes form

$$\mathcal{B}_{n+1}^+ = \frac{2\mathcal{K}_{n+1}}{\sin\gamma_{n+1}} + \frac{\mathcal{B}_n^+}{1 + \tau_n \mathcal{B}_n^+},$$

where $\mathcal{K}_{n+1}$ is the curvature of the boundary $\partial\mathcal{D}$ at the point (x_{n+1}, y_{n+1}):

$$\mathcal{K}_{n+1} = \frac{f_1''(x_{n+1})}{\bigl(1 + [f_1'(x_{n+1})]^2\bigr)^{3/2}} = a_1 + \mathcal{O}(x_{n+1}).$$

The recurrence formula (4.11) changes accordingly:

$$\lambda_{n+1} = \frac{2\tau_{n+1}\mathcal{K}_{n+1}}{\sin\gamma_{n+1}} + \frac{\tau_{n+1}}{\tau_n}\,\frac{\lambda_n}{1 + \lambda_n}. \tag{6.8}$$

We observe two new elements here, as compared to (4.11) of Section 4: there is an extra factor of $\bar{a}$ in the denominator, due to (6.7), and an extra factor $a_1 + \mathcal{O}(x_n)$ in the numerator due to the curvature. Of course, when the collision occurs at the other side of the cusp, the curvature will be $a_2 + \mathcal{O}(x_n)$.

As the trajectory collides alternatively at both sides, the extra factors a_1 and a_2 alternate in the numerator. Due to the additive character of (6.8), the combined effect of the extra factors a_1 and a_2 in the numerator will be exactly opposite to that of the extra factor of $\bar{a} = (a_1 + a_2)/2$ in the denominator, so in the end all the new factors will cancel out. This proves Proposition 4.1 in the general case.

Lastly we extend the results of Section 5 to the general case. Our main task is to describe the structure of the cells E_N. Let P denote the vertex of a cusp and L the common tangent line to the two boundary components making the cusp. Let $Q(P)$ denote the other point of intersection of L with $\partial\mathcal{D}$ (opposite to P). For example, on Fig. 1 we have $D = Q(A)$.

In generic billiard tables, L intersects $\partial\mathcal{D}$ at Q transversally, then, just as in Section 5, points $x \in E_N$ whose trajectories enter the cusp have to start near Q and their images $\hat{\mathcal{F}}(x) = \mathcal{F}^{N+1}(x)$ have to land back near Q again. Of course the φ-coordinate of $x \in E_N$ and $\mathcal{F}^{N+1}(x) \in F_N$ need not be close to zero, so the cells E_N may lie far away from their images F_N. But all the estimates of Section 5 obviously remain valid.

In the exceptional case, where the line L is tangent to $\partial\mathcal{D}$ at the point Q, the analysis requires modification. The boundary $\partial\mathcal{D}$ may be smooth at Q (thus L makes a 'grazing collision' at the point Q), or Q itself may be a corner point or even another cusp (!). For example, imagine a diamond-looking table made by four identical circular arcs tangent to each other at their endpoints – there are two pairs of cusps opposite to each other.

In these exceptional cases one can analyze the cell structure directly, but this may be fairly complicated. A useful trick, however, may reduce the analysis to the generic case, in which the line L intersects $\partial\mathcal{D}$ transversally. One simply adds to $\partial\mathcal{D}$ a short 'transparent' line segment positioned inside $\mathcal{D}$ so that it cuts L transversally (or even orthogonally) between the points P and Q. We note that adding transparent walls to billiards is a standard trick [SC87].

Now the billiard trajectories going into the cusp for long corner series must first cross that newly added segment. They do not change their velocities (the segment is transparent, after all), but we register the point of intersection as an extra collision point. Therefore all the cells E_N will appear on that extra segment added to the boundary. Their parameters will be obviously the same as described in Section 5. This allows us to prove Theorem 1.1 in the exceptional cases.

We conclude with an open problem. We always assumed that the curvature of the boundary $\partial\mathcal{D}$ did not vanish, in particular we had $a_1, a_2 > 0$ in this section. It is interesting to let the curvature vanish at the vertex of the cusp, so that $a_1 = 0$ or $a_2 = 0$, or both. Would this affect the rate of the decay of correlations?

It seems that if $a_1 = 0$ but $a_2 > 0$ (or vice versa), then the rate will not change. But in the case $a_1 = a_2 = 0$ the cusp becomes very degenerate and may trap billiard trajectories for much longer than 'regular' cusps treated here. This may slow down the decay of correlations even further. A similar phenomenon was recently discovered in [CZ05b].

Acknowledgement. We thank our colleagues P. Balint, D. Dolgopyat, and H.-K. Zhang for many useful discussions and Alvaro Pardo for assisting us with computer simulations. N. Ch. was partially supported by NSF grant DMS-0354775. R. M. was partially supported by the Proyecto PDT 29/219 (CONICYT, Uruguay).

References

[BG06] P. Bálint & S. Gouëzel, *Limit theorems in the stadium billiard*, Comm. Math. Phys. **263** (2006), 461–512.

[BS81] L. A. Bunimovich & Ya. G. Sinai, *Statistical properties of Lorentz gas with periodic configuration of scatterers*, Comm. Math. Phys. **78** (1981), 479–497.

[BSC90] L. A. Bunimovich, Ya. G. Sinai & N. I. Chernov, *Markov partitions for two-dimensional billiards*, Russ. Math. Surv. **45** (1990), 105–152.

[BSC91] L. A. Bunimovich, Ya. G. Sinai & N. I. Chernov, *Statistical properties of two-dimensional hyperbolic billiards*, Russ. Math. Surv. **46** (1991), 47–106.

[C99] N. Chernov, *Decay of correlations and dispersing billiards*, J. Statist. Phys. **94** (1999), 513–556.

[C06a] N. Chernov, *Regularity of local manifolds in dispersing billiards*, Math. Phys. Electr. J. **1** (2006), 54 pp.

[C06b] N. Chernov, *Advanced statistical properties of dispersing billiards*, J. Statist. Phys., to appear.

[CH96] N. Chernov & C. Haskell, *Nonuniformly hyperbolic K-systems are Bernoulli*, Ergod. Th. Dynam. Syst. **16** (1996), 19–44.

[CD06] N. Chernov & D. Dolgopyat, *Brownian Brownian Motion – I*, manuscript; available at http://www.math.uab.edu/chernov/papers/pubs.html

[CZ05a] N. Chernov & H.-K. Zhang, *Billiards with polynomial mixing rates*, Nonlinearity **18** (2005), 1527–1553.

[CZ05b] N. Chernov & H.-K. Zhang, *A family of chaotic billiards with variable mixing rates*, Stochastics & Dynamics **5** (2005), 535–553.

[CM06] N. Chernov & R. Markarian, *Chaotic Billiards*, AMS, to appear.

[CGS92] P. Collet, A. Galves, & B. Schmitt, *Unpredictability of the ocurrence time of a long laminar laminar period in a model of temporal intermittency*, Ann. Inst. H. Poincaré. Phys. Théor. **57** (1992), 319–331.

[CG93] P. Collet & A. Galves, *Statistics of Close Visits to the Indifferent Fixed Point of an Interval Map*, J. Statist. Phys **72** (1993), 459–478.

[GO74] G. Gallavotti & D. S. Ornstein, *Billiards and Bernoulli Schemes*, Comm. Math. Phys. **38** (1974), 83-101.

[Mac83] J. Machta, *Power law decay of correlations in a billiard problem*, J. Statist. Phys. **32** (1983), 555–564.

[MR86] J. Machta & B. Reinhold, *Decay of correlations in the regular Lorentz gas*, J. Statist. Phys. **42** (1986), 949–959.

[Mar04] R. Markarian, *Billiards with polynomial decay of correlations*, Ergod. Th. Dynam. Syst. **24** (2004), 177–197.

[OW98] D. Ornstein & B. Weiss, *On the Bernoulli nature of systems with some hyperbolic structure*, Ergod. Th. Dynam. Syst. **18** (1998), 441–456.

[R95] J. Reháček, *On the ergodicity of dispersing billiards*, Rand. Comput. Dynam. **3** (1995), 35–55.

[Si70] Ya. G. Sinai, *Dynamical systems with elastic reflections. Ergodic properties of dispersing billiards*, Russ. Math. Surv. **25** (1970), 137–189.

[SC87] Ya. G. Sinai and N. I. Chernov, *Ergodic properties of some systems of 2-dimensional discs and 3-dimensional spheres*, Russ. Math. Surv. **42** (1987), 181–207.

[Y98] L.-S. Young, *Statistical properties of dynamical systems with some hyperbolicity*, Ann. Math. **147** (1998), 585–650.

[Y99] L.-S. Young, *Recurrence times and rates of mixing*, Israel J. Math. **110** (1999), 153–188.